A Ca^{2+}-induced Ca^{2+} Release Mechanism Involved in Asynchronous Exocytosis at Frog Motor Nerve Terminals

K. Narita,[§] T. Akita,* M. Osanai,[‖] T. Shirasaki,[‡¶] H. Kijima,** and K. Kuba*[‡]

From the *Department of Physiology, School of Medicine, Nagoya University, Showa-ku, Nagoya 466-8550, Japan; [‡]Department of Physiology, Saga Medical School, Saga 849-8501, Japan; [§]Department of Physiology, Kawasaki Medical School, Kurashiki 701-0192, Japan; [‖]Department of Pharmacology, Tokyo Medical and Dental University, School of Medicine, Tokyo 113-8519, Japan; [¶]Department of Physiology, Kansai Medical University, Moriguchi 570-0074, Japan; and **Department of Physics, School of Science, Nagoya University, Nagoya 464-8602, Japan

ABSTRACT The extent to which Ca^{2+}-induced Ca^{2+} release (CICR) affects transmitter release is unknown. Continuous nerve stimulation (20–50 Hz) caused slow transient increases in miniature end-plate potential (MEPP) frequency (MEPP-hump) and intracellular free Ca^{2+} ($[Ca^{2+}]_i$) in presynaptic terminals (Ca^{2+}-hump) in frog skeletal muscles over a period of minutes in a low Ca^{2+}, high Mg^{2+} solution. Mn^{2+} quenched Indo-1 and Fura-2 fluorescence, thus indicating that stimulation was accompanied by opening of voltage-dependent Ca^{2+} channels. MEPP-hump depended on extracellular Ca^{2+} (0.05–0.2 mM) and stimulation frequency. Both the Ca^{2+}- and MEPP-humps were blocked by 8-(*N,N*-diethylamino)octyl3,4,5-trimethoxybenzoate hydrochloride (TMB-8), ryanodine, and thapsigargin, but enhanced by CN^-. Thus, Ca^{2+}-hump is generated by the activation of CICR via ryanodine receptors by Ca^{2+} entry, producing MEPP-hump. A short interruption of tetanus (<1 min) during MEPP-hump quickly reduced MEPP frequency to a level attained under the effect of TMB-8 or thapsigargin, while resuming tetanus swiftly raised MEPP frequency to the previous or higher level. Thus, the steady/equilibrium condition balancing CICR and Ca^{2+} clearance occurs in nerve terminals with slow changes toward a greater activation of CICR (priming) during the rising phase of MEPP-hump and toward a smaller activation during the decay phase. A short pause applied after the end of MEPP- or Ca^{2+}-hump affected little MEPP frequency or $[Ca^{2+}]_i$, but caused a quick increase (faster than MEPP- or Ca^{2+}-hump) after the pause, whose magnitude increased with an increase in pause duration (<1 min), suggesting that Ca^{2+} entry-dependent inactivation, but not depriming process, explains the decay of the humps. The depriming process was seen by giving a much longer pause (>1 min). Thus, ryanodine receptors in frog motor nerve terminals are endowed with Ca^{2+} entry-dependent slow priming and fast inactivation mechanisms, as well as Ca^{2+} entry-dependent activation, and involved in asynchronous exocytosis. Physiological significance of CICR in presynaptic terminals was discussed.

KEY WORDS: intracellular calcium • Ca^{2+} influx • ryanodine receptor • transmitter release

INTRODUCTION

Ca^{2+} in presynaptic terminals plays key roles not only in the impulse-induced exocytosis of neurotransmitters, but also in other slow regulatory actions on transmitter release, such as the turnover of synaptic vesicles and short- and long-term plasticities (see Katz, 1969; reviewed by Schweizer et al., 1995; Südhof, 1995; Zucker, 1996). While impulse-induced release of transmitter appears to be caused by a high $[Ca^{2+}]_i$ existing in a short period at the orifice of voltage-activated Ca^{2+} channels (Llinás et al., 1992; Heidelberger et al., 1994; Landò and Zucker, 1994), slow regulatory actions of Ca^{2+} could result from a longer, more global, but moderate rise in cytosolic Ca^{2+} concentration ($[Ca^{2+}]_i$), as has been well known for the action of residual $[Ca^{2+}]_i$ remaining after preceding impulses on short-term plasticities of transmitter release (Katz and Miledi, 1968; Tanabe and Kijima, 1992; see Zucker, 1996).

Such a moderate, prolonged increase in $[Ca^{2+}]_i$, however, could more effectively be achieved by the release of Ca^{2+} from intracellular Ca^{2+} stores in response to impulses (see review by Kuba, 1994). Erulkar and Rahamimoff (1978) suggested that tetanic and post-tetanic increases in miniature end-plate potential (MEPP)[1] frequency in a Ca^{2+}-free (EGTA) solution are the result of intracellular Ca^{2+} release activated by Na^+ entering

Portions of this work were previously published in abstract form (Narita, K., K. Kuba, T. Mitsumoto, T. Shirasaki, M. Osanai, and H. Kijima. 1996. *Neurosci. Res.* 20:S49).

Address correspondence to Dr. Kenji Kuba, Department of Physiology, School of Medicine, Nagoya University, 65 Tsurumai-cho, Showa-ku, Nagoya 466-8550, Japan. Fax: +81-52-744-2049; E-mail: kubak@med.nagoya-u.ac.jp

[1]*Abbreviations used in this paper:* CICR, Ca^{2+}-induced Ca^{2+} release; IP_3, inositoltrisphosphate; MEPP, miniature end-plate potential; TMB-8, 8-(*N,N*-diethylamino)octyl3,4,5-trimethoxybenzoate hydrochloride.

during nerve impulses. On the other hand, much evidence has been accumulated that the activation of Ca^{2+}-induced Ca^{2+} release (CICR) via ryanodine receptors occurs in response to Ca^{2+} entry in the cell soma and dendrites of neurones (Kuba and Nishi, 1976; Kuba, 1980; Thayer et al., 1988; Lipscombe et al., 1988; Friel and Tsien, 1992; Llano et al., 1994; Garaschuk et al., 1997; see review by Kuba, 1994). The evidence, however, for the involvement of CICR in exocytosis at presynaptic terminals is rather indirect. Caffeine and theophylline, activators of ryanodine receptor, have been known to enhance both the evoked and spontaneous release of transmitters in several types of terminals, including frog motor nerve terminals (Elmqvist and Feldman, 1965; Onodera, 1973; Ohta and Kuba, 1980; Lockerbie and Gordon-Weeks, 1986; Tóth et al., 1990). Recent studies suggested ryanodine-sensitive components of tetanus-induced rise in $[Ca^{2+}]_i$ and transmitter release in autonomic nerve terminals (Peng, 1996; Smith and Cunnane, 1996).

In this study, we have tested the hypothesis that Ca^{2+} entry produced by impulses activates CICR in presynaptic terminals, amplifies the rise in $[Ca^{2+}]_i$, and enhances transmitter release and other Ca^{2+}-dependent functions. We have measured changes in the frequency of MEPPs and $[Ca^{2+}]_i$ in motor nerve terminals in response to tetanic stimulation in combination with pauses in tetanus of various duration and timing at frog neuromuscular junctions and observed effects of blockers of Ca^{2+} release and uptake. The results suggest that CICR occurs via the activation of ryanodine receptors in response to Ca^{2+} entries accompanying impulses and enhances asynchronous release of transmitter. They further revealed unique Ca^{2+} entry-dependent priming, depriming, inactivation, and deinactivation processes of ryanodine receptors as well as Ca^{2+} entry-dependent activation process. The CICR mechanism, which is normally deprimed under the resting condition, is slowly primed, subsequently activated, and then inactivated by Ca^{2+} entry accompanying nerve activity, and eventually deprimed slowly in the absence of Ca^{2+} entry.

MATERIALS AND METHODS

Electrophysiology

Frogs (*Rana nigromaculata*) were decapitated and sartorius muscles with the innervating nerve were isolated. Most experiments were carried out after the incubation of preparations at 4°C for 3–12 h to place them in a condition similar to that for measurement of $[Ca^{2+}]_i$. Such a treatment did not essentially affect the amplitude and time course of changes in MEPP frequency in response to continuous tetanus. The composition of normal Ringer's solution (mM) was 100 NaCl, 2 KCl, 2.5 $CaCl_2$, 3.0 $MgCl_2$, 8.0 Tris, pH 7.4. Low Ca^{2+}, high Mg^{2+} solutions were made by lowering $CaCl_2$ (0.02–0.2 mM) and adding $MgCl_2$ (10 mM) with the adjustment of osmolarity by changing NaCl concentration. A Ca^{2+}-free (EGTA), Mg^{2+} solution was made by removing $CaCl_2$ and adding 1 mM $MgCl_2$ and 1 mM EGTA. Neostigmine bromide (10^{-6} g/ml) was added to all solutions to enhance the amplitude of MEPP for the accurate measurement of its frequency. MEPPs were recorded by a conventional intracellular recording technique using electrodes filled with 3 M KCl at 20–24°C. They were stored on a PCM recorder (40 kHz, RD101T or RD125T; TEAC, Tokyo, Japan) and fed into a computer (PC-9801-DA, NEC; Tokyo, Japan) through a GPIB interface (GP-300 or GP-350; TEAC) that also controlled the transfer of the data into the computer memory. All the digitized MEPPs were low-pass filtered at 5 kHz (six poles, Butterworth; installed in RD101T and RD125T). In most analyses, MEPPs displayed on the screen were identified by eye and their number was counted. When the summation of MEPPs was so large that the number of MEPPs buried in the record could not be ignored (usually >200/s), MEPP frequency was estimated from the integration of voltage records (Mulkey and Zucker, 1993). The voltage record was divided into 1-s segments. The areas enclosed by the voltage trace in each segment and the base line measured before the beginning of tetanus were integrated. To eliminate the contribution of stimulation artifacts, the record of one segment that contained artifacts but not MEPP was integrated and subtracted from the integration of the record that contained MEPPs. The result was divided by the area of the averaged single MEPP (or the product of the mean amplitude and the sum of the decay time constant and the rise time) recorded discretely at low frequency, yielding MEPP frequency. A blocker of ryanodine receptor, 8-(*N,N*-diethylamino)octyl3,4,5-trimethoxybenzoate hydrochloride (TMB-8), reduced the amplitude of MEPP to 81% of the control (see also Hunt et al., 1990). This action, however, did not affect the estimation of MEPP frequency for the following reasons. First, the extent of the decrease in MEPP amplitude was not large enough to affect identification by eye. Second, both the voltage trajectory of summated MEPPs and a single MEPP should be similarly affected by TMB-8 so that their division could be unchanged.

$[Ca^{2+}]_i$ Measurements

Changes in $[Ca^{2+}]_i$ in frog motor nerve terminals were measured from those of cutaneous pectoris muscles. Frogs were decapitated and cutaneous pectoris muscles with the innervating nerve were isolated. The composition of normal Ringer's solution (mM) was 112 NaCl, 2 KCl, 1.8 $CaCl_2$, 2.4 $NaHCO_3$, pH 7.4 (when equilibrated with air), with or without 5.0 glucose or 111 NaCl, 2 KCl, 1.8 $CaCl_2$, 5.0 Hepes-Na, pH 7.4, 5.0 glucose. Low Ca^{2+}, high Mg^{2+} and Ca^{2+}-free (EGTA), Mg^{2+} solutions were prepared similarly as in the experiments for recording MEPPs. K-salt of Indo-1, Oregon Green BAPTA-1, or Fura-2 was loaded into the terminals from the cut end of the nerve bundle (Peng and Zucker, 1993). A drop (0.2–0.5 μl) of a Ca^{2+}-free solution (buffered with 10 mM HEPES-Na, pH 7.4) containing K-salt of Indo-1, Oregon Green BAPTA-1, or Fura-2 (30 mM) was placed at the cut end of the nerve in a moist chamber and incubated for 8–12 h at 20–22°C (Osanai et al., 1996). During this period, Ca^{2+} probes were transported or diffused through the axon cytoplasm down to the terminals. In most experiments, cutaneous pectoris muscles, whose nerve terminals were loaded with Ca^{2+} probes, were set on a plastic plate, which was held upside down in a recording chamber placed on the stage of an inverted microscope (TMD or TMD-300; objective, 40× water/N.A. 1.15; Nikon, Tokyo, Japan). The innervating nerves were stimulated with a pair of platinum wires set in a plastic tube attached to the plate, on which the muscles were fixed.

There are two reasons for the use of different preparations for recording MEPPs and $[Ca^{2+}]_i$ in nerve terminals. First, we have

initially started the experiments by recording MEPPs from frog sartorius muscles and most data that suggest the existence of CICR in nerve terminals were obtained from measurement of MEPPs. Second, small, thin muscle preparations, such as cutaneous pectoris muscles, were relevant for recording fluorescence from the motor nerve terminals of neuromuscular preparations with an inverted microscope. Limitations for the use of different preparations and the rationale that the data obtained from independent experiments on different preparations could lead to the conclusion of the present study are described in the DISCUSSION.

In most experiments, confocal laser scanning microscopes (MRC-500 or -600; Nippon Biorad, Tokyo, Japan) equipped with an ultraviolet Argon laser (351 nm; Kuba et al., 1994) or Krypton-argon laser (488 nm) were used to measure fluorescence changes of Indo-1 or Oregon Green BAPTA-1. Indo-1 fluorescence intensity was measured at two wavelength ranges separated at 445 nm and the ratio of fluorescence (F_{412}/F_{475}) was converted to a $[Ca^{2+}]_i$ value using Eq. 5, described by Grynkiewicz et al. (1985). The apparent dissociation constant, the maximum and minimum ratios for conversion were obtained from the relationship in vitro between the ratio of Indo-1 fluorescence and the known concentration of Ca^{2+} in a pseudo-intracellular solution (140 mM KCl, 10 mM EGTA, 10–25 μM Indo-1, 10 mM HEPES-K, pH.7.2, and various concentrations of $CaCl_2$) containing aldolase (2–4 mg/ml, Type IV; Sigma Chemical Co., St. Louis, MO), which was assumed to mimic endogenous cytosolic proteins affecting a Ca^{2+} dependence of Indo-1 fluorescence (Konishi et al., 1988). The dissociation constant of Indo-1 was found to be ~450 nM in the presence of 2–4 mg/ml aldolase, about twice that in a protein-free solution. Since both maximum and minimum ratios were reported to depend on the concentration and type of proteins (Baker et al., 1994), absolute values of $[Ca^{2+}]_i$ estimated would be subject to ambiguity by a factor of 2. Nevertheless, this possible error would have little effect on the interpretation of the results throughout this paper. In the analyses of fluorescence images of Oregon Green BAPTA-1, the ratios of the images during and after nerve stimulation to that before stimulation (F/F_C) were taken. This corrected differences in path length and dye concentration variation (Neher and Augustine, 1992). Ratios were converted to $[Ca^{2+}]_i$ values by the equation expressing the relationship between Ca^{2+} concentration and F/F_C.

$$[Ca^{2+}]_i = K_d (AF/F_C - 1) / (F_{max}/F_{min} - AF/F_C),$$

where $A = (F_{max}/F_{min} + K_d/[Ca^{2+}]_C) / (1 + K_d/[Ca^{2+}]_C)$, F_{max}, and F_{min} are the maximum and minimum fluorescence intensities, respectively, of Oregon Green BAPTA-1 at a high (enough to saturate the probe) and zero concentration of Ca^{2+}, respectively, and $[Ca^{2+}]_C$ was the $[Ca^{2+}]_i$ before stimulation. The values for $[Ca^{2+}]_C$ and the K_d of Oregon Green BAPTA-1 used in calculation were 72 ± 9 nM (n = 18; previously obtained from Indo-1 fluorescence measurement) and 240 nM (obtained similarly as in the case of Indo-1; our unpublished observations), respectively. The values for F_{max} and F_{min} were obtained in vitro by measuring the fluorescence intensities of pseudo-intracellular solutions containing 10 μM Ca^{2+} and no Ca^{2+}, respectively, and their ratio was found to be 15.0.

Scanning of the nerve terminals was made by an x–y scan mode with or without the summation of two to four images. The averages of the ratios of Indo-1 fluorescence or the intensities of Oregon Green fluorescence were measured from small areas (2.25–4 μm^2) of the images of individual terminals.

In some experiments, examining quenching effects of Mn^{2+} on fluorescence of Fura-2 loaded in nerve terminals, the fluorescence was measured with a cooled CCD-camera (Argus/HiSca, C6790-81; Hamamatsu Photonics, Hamamatsu, Japan) through an image intensifier attached to an upright microscope (Zeiss Axioscope, objective 100× water/N.A. 0.95; Carl Zeiss Japan, Tokyo, Japan) and analyzed by image analysis software (Argus; Hamamatsu Photonics).

Statistical Tests

Student's *t* tests were made for the data in which they were apparently required.

Drugs

Indo-1/K, Oregon Green BAPTA-1/K, and Fura-2/K were obtained from Molecular Probes, Inc. (Eugene, OR). TMB-8 was from Sigma Chemical Co. (St. Louis, MO) or Tokyo Kasei Kogyo Co. (Tokyo, Japan). Ryanodine, HEPES-Na or -K, aldolase, and neostigmine bromide were from Sigma Chemical Co. Thapsigargin was from Research Biochemicals, Inc. (Natick, MA) or Sigma Chemical Co.

Experimental Parameters Reflecting the Rate of Ca^{2+} Release

The approximate estimation of changes in the rate of Ca^{2+} release from changes in $[Ca^{2+}]_i$ and MEPP frequency was made based on a simple model for intracellular Ca^{2+} dynamics (Fig. 1). Ca^{2+} diffusion can be neglected in the formation of rate equations for Ca^{2+} dynamics in response to Ca^{2+} entry and Ca^{2+} release, since most changes recorded in $[Ca^{2+}]_i$ were much slower than the time for spatial equilibrium of Ca^{2+}, and the $[Ca^{2+}]_i$ values measured are the average over those within a small region (a few square micrometers) of the terminal. It is further assumed that the rates of Ca^{2+} binding to, and unbinding from, proteins are so fast that the reactions can be considered to be at equilibrium (Neher and Augustine, 1992). Likewise, the rates of Ca^{2+} uptake into, and release from, mitochondria are assumed to be faster than those of other Ca^{2+} stores. This assumption can be supported by similar time courses of Ca^{2+}-humps in the absence and presence of CN^- (see Fig. 6 *C*). Then, the rate of changes in $[Ca^{2+}]_i$ (dx/dt) is expressed by the sum of the rates of Ca^{2+} entry during tetanus (J_{Ca}*), Ca^{2+} release from Ca^{2+} stores (γz), Ca^{2+} uptake into Ca^{2+} stores (αx), and Ca^{2+} extrusion at the cell mem-

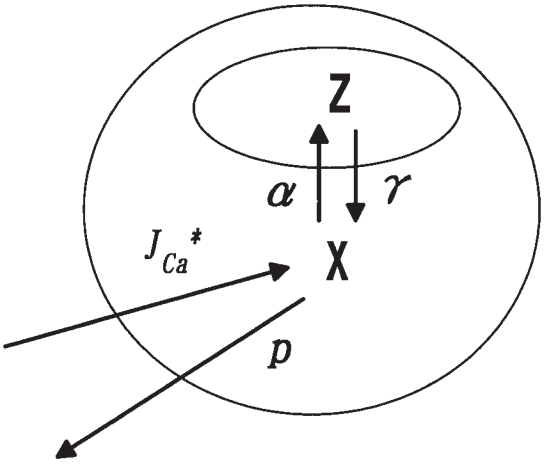

FIGURE 1. A scheme to illustrate Ca^{2+} dynamics involving CICR in frog motor nerve terminals. Ca^{2+} enters into the motor nerve terminals through voltage-dependent Ca^{2+} channels (J_{Ca}*), and is extruded out of the terminal by Ca^{2+} pumps (p) at the cell membrane. Cytoplasmic Ca^{2+} (x) activates Ca^{2+} release (γ) from Ca^{2+} stores and is taken into Ca^{2+} stores (z) by Ca^{2+} pumps (α) to resume Ca^{2+} concentration in Ca^{2+} stores.

brane (px). Thus, an equation similar to that previously proposed for CICR (Kuba and Takeshita, 1981) was derived with the inclusion of Ca^{2+} buffering by Ca^{2+} binding proteins and mitochondria ($1 + \kappa_s$):

$$(1 + \kappa_s)\, dx/dt = J_{Ca}^* + \gamma z - (\alpha + p)\, x \quad (1)$$

or

$$\gamma z = (1 + \kappa_s)\, dx/dt + (\alpha + p)\, x - J_{Ca}^*, \quad (2)$$

where x and z are $[Ca^{2+}]_i$ and the Ca^{2+} concentration of Ca^{2+} stores ($[Ca^{2+}]_s$), respectively, γ, p, and α are rate constants, and κ_s is the sum of the Ca^{2+} binding capacity of endogenous Ca^{2+} binding proteins (Neher and Augustine, 1992) and the Ca^{2+} uptake capacity of mitochondria. In the equation, Ca^{2+} influx into Ca^{2+} stores through Ca^{2+} release channels was implicitly ignored. The rate constants, γ, p, and α, include the total number of Ca^{2+} release channels (for γ) or Ca^{2+} pumps (for p and α), open probability of Ca^{2+} release channels (for γ) or rate constants of the single Ca^{2+} pump (for p and α), and the volume of the free cytoplasm or Ca^{2+} stores (for γ and p, respectively). J_{Ca}^* is a function of the total number, open probability, and permeability of Ca^{2+} channels, the extracellular Ca^{2+} concentration, cell membrane potential, and the total volume of cytoplasm. It may safely be assumed that J_{Ca}^* is constant, since Ca^{2+}-dependent inactivation of voltage-dependent Ca^{2+} channels appears to be not so large, if it occurs, as suggested from the quick quenching effect of Mn^{2+} (see Fig. 4). Furthermore, J_{Ca}^* in low Ca^{2+} (0.05–0.2 mM), high Mg^{2+} (10 mM) solutions used in the present study is negligibly small when compared with the net rate of Ca^{2+} release ($\gamma z - \alpha x$), seen as a transient rise in $[Ca^{2+}]_i$ (see Figs. 3 and 10 *A*). Then, Eq. 2 implies that the sum of $(1 + \kappa_s)\, dx/dt$ and $(\alpha + p)\, x$ would reflect the rates of Ca^{2+} release.

When $(\alpha + p)\, x$ is much greater than $(1 + \kappa_s)\, dx/dt$ (or dx/dt is negligibly small: steady/equilibrium approximation; Kijima and Kijima, 1982), it becomes,

$$\gamma z \approx (\alpha + p)\, x. \quad (3)$$

On the other hand, when $(\alpha + p)\, x$ is smaller than $(1 + \kappa_s)\, dx/dt$,

$$\gamma z \approx (1 + \kappa_s)\, dx/dx. \quad (4)$$

When the values of dx/dt are measured at similar values of x, changes in dx/dt would reflect changes in the rate of Ca^{2+} release (see Eq. 2).

In addition to $[Ca^{2+}]_i$ measurement, we have used changes in MEPP frequency as a reflection of changes in $[Ca^{2+}]_i$ with the understanding that MEPP frequency depends on the power of $[Ca^{2+}]_i$ (Ravin et al., 1997), the efficiency of exocytosis, and the amount of transmitter available for release. The amount of transmitter pool may be decreased by an increase in MEPP frequency during tetanus. Such a reduction, however, would have been ~300–500 quanta/s, assuming that each MEPP consists of a single quantum. This is roughly equivalent to that caused by the stimulation at 2 Hz in normal Ringer solution, since 200 quanta are usually released by a nerve impulse at frog motor nerve terminals (Gage, 1976). Thus, the reduction of available pools of transmitter may be negligible. On the other hand, the efficiency of exocytosis may change during continuous tetanic stimulation. This indeed took place in the present experiments. Changes in MEPP frequency due to alterations in exocytotic efficiency, however, were relatively small when compared with those produced by CICR (Fig. 2 *D*). This conventional interpretation of MEPP frequency may therefore be used in the analyses of CICR. In fact, the time course of changes in MEPP frequency and $[Ca^{2+}]_i$ in response to tetanus, its interruption, and actions of blockers of Ca^{2+} release and uptake were similar. However, the extent of changes in MEPP frequency exceeded those for $[Ca^{2+}]_i$ due to the power law dependence of MEPP frequency on $[Ca^{2+}]_i$.

RESULTS

All the experiments were done in low Ca^{2+} (0.05–0.2 mM), high Mg^{2+} (10 mM) or Ca^{2+}-free (EGTA), and Mg^{2+} (1 mM) solutions, where no end-plate potentials were evoked by nerve stimulation (Fig. 2 *A*). Under this condition, the contribution of CICR to impulse-induced rise in $[Ca^{2+}]_i$ would be greater, if it occurs. MEPPs were recorded from the end plates of frog sartorius muscles, while changes in $[Ca^{2+}]_i$ were measured from the motor nerve terminals of frog cutaneous pectoris muscles.

A Transient Increase in MEPP Frequency during Continuous Tetanic Stimulation

Continuous nerve stimulation at 50 Hz produced a large transient rise in MEPP frequency (MEPP-hump) in frog sartorius muscles. The MEPP-hump grew over a few minutes, reached a peak (288.0 ± 43.6/s, SEM, n = 17 from the resting value of 0.58 ± 0.13/s, n = 17, $P <$ 0.001) and decayed to a level (77.6 ± 8.4/s, n = 17, $P <$ 0.001 when compared with the resting value) higher than the control at a rate slightly faster than that of growth (Fig. 2, *A* and *B*). This was followed by a slow progressive rise (122.0 ± 26.5/s, n = 14, at 2 min after the end of a transient rise, $P < 0.2$ when compared with that immediately after the MEPP-hump; Fig. 2, *A* and *B*). Decreasing tetanus frequency to 20 Hz reduced the magnitude of MEPP-hump and delayed its peak (Fig. 2 *C*). Lowering $[Ca^{2+}]_o$ from 0.2 to 0.1 mM reduced MEPP-hump to 76.7 ± 13.2/s (n = 8, $P < 0.001$), and the later slow rise in MEPP frequency to 66.6 ± 9.5/s (n = 8, $P < 0.2$; Fig. 2 *B*). MEPP-hump was almost abolished at 0.05 mM $[Ca^{2+}]_o$. It may be noted that the strong potentiation of exocytotic mechanism may also occur in the late slow rise in MEPP frequency. The mechanism for this slow rise was not studied here, although it is of interest.

A Transient Rise in $[Ca^{2+}]_i$ in Motor Nerve Terminals during a Tetanus

Continuous tetanic stimulation (50 Hz) also caused a transient increase in $[Ca^{2+}]_i$ in motor nerve terminals (Ca^{2+}-hump) in frog cutaneous pectoris muscles. Changes in $[Ca^{2+}]_i$ were measured by recording alterations in the fluorescence ratio of Indo-1 or Oregon Green BAPTA-1 in a region (a few square micrometers) of the images of the terminals. The Ca^{2+}-hump recorded with Indo-1 fluorescence rose in a few minutes to peak (from 69 ± 8 nM to 1.58 ± 0.2 μM, n = 12; $P <$ 0.001) and decayed to a level (320 ± 14 nM; $P < 0.001$ when compared with the resting value) higher than

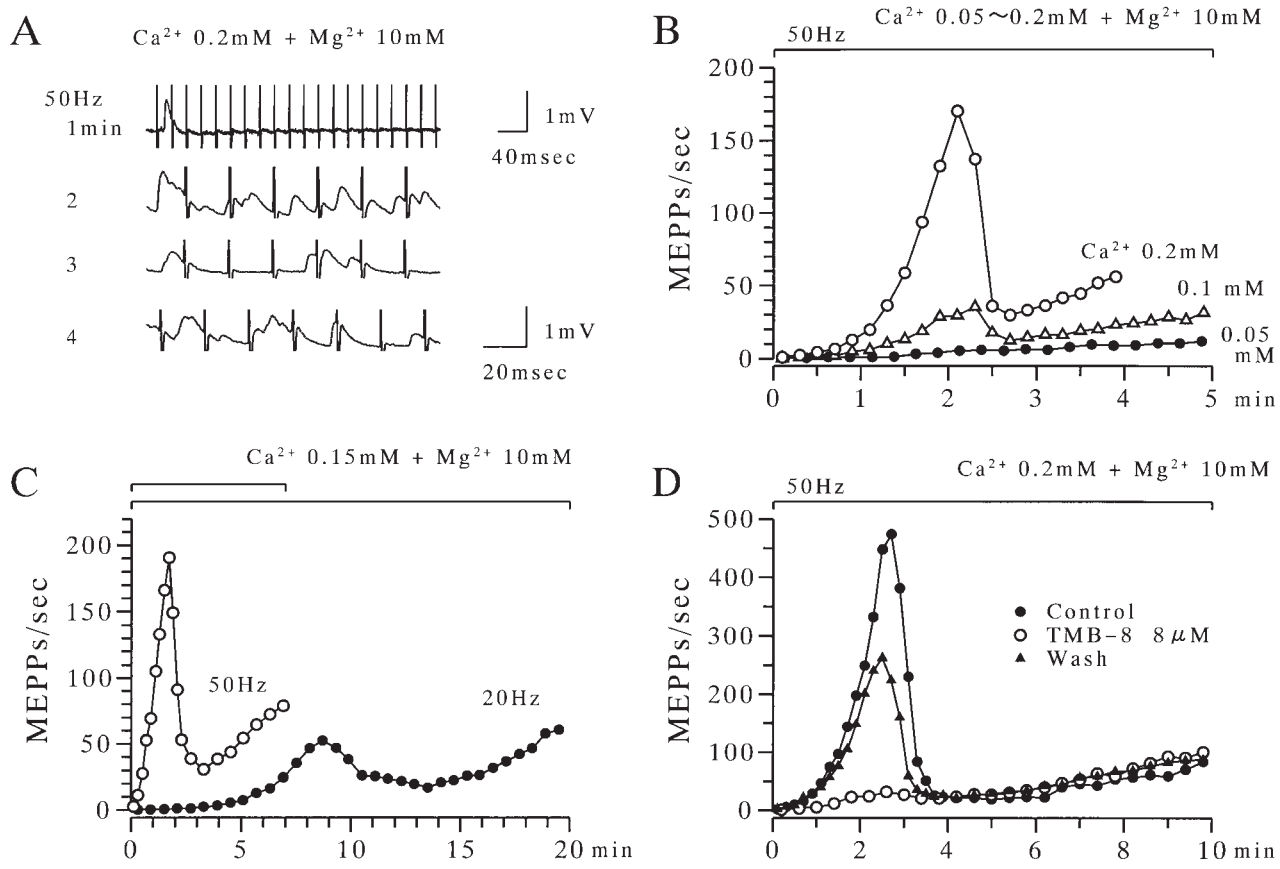

FIGURE 2. Tetanus-induced transient increases (MEPP-hump) and late slow rises in MEPP frequency in a low Ca^{2+}, high Mg^{2+} solution. Tetanus at 50 Hz (except for one of the data in *C*) was continuously applied throughout each experiment. (*A*) MEPPs recorded at 1 (at the beginning of MEPP-hump shown in *B*), 2 (at the peak of MEPP-hump), 3 (at the end of MEPP-hump), and 4 (during a late slow rise) min after the beginning of a continuous tetanus (50 Hz) in a low Ca^{2+} (0.2 mM), high Mg^{2+} (10 mM) solution. (*B*) Time courses of MEPP-hump and the late slow rise in MEPP frequency produced by a continuous tetanus (50 Hz) and effects of lowering $[Ca^{2+}]_o$. $[Ca^{2+}]_o$ was reduced from 0.2 mM (○; control) to 0.1 (Δ) or 0.05 (●) mM. (*C*) Effects of decreasing tetanus frequency on MEPP-humps. (*D*) Effects of TMB-8 (8 μM) on MEPP-humps and late slow rises in MEPP frequency. After recording the control response, the preparation was left for 30 min without nerve stimulation. Then, a solution containing TMB-8 was superfused to the preparation for 30 min and a tetanus (50 Hz) was given. MEPPs were again recorded 1 h after the removal of TMB-8.

that before stimulation (Figs. 3 and 4 *A*). Ratio images of Oregon Green BAPTA-1 fluorescence showed a better signal to noise ratio (Fig. 5). Ca^{2+}-humps measured by Oregon Green BAPTA-1 fluorescence were in general similar in time course and space, but varied to some extent in amplitude (see also Fig. 10 *A*).

Ca^{2+}-humps were blocked by lowering $[Ca^{2+}]_o$ (not shown). The time course of Ca^{2+}-hump resembled that of MEPP-hump, although the magnitude of relative changes to that before stimulation was much greater in the latter (obviously for the power law dependence of MEPP frequency on $[Ca^{2+}]_i$). The results suggest that similar mechanisms underlie in both MEPP- and Ca^{2+}-humps, although the activation of the exocytotic process is also involved in the former.

Ca^{2+}-hump was followed by the late slow rise in $[Ca^{2+}]_i$, which was maintained further (354 ± 17 nM at 2 min; $P < 0.001$ in respect to the $[Ca^{2+}]_i$ before stimulation, $P < 0.2$ when compared with that immediately after the Ca^{2+}-hump). The magnitudes of the late slow rises in $[Ca^{2+}]_i$ were variable among terminals and smaller than those of MEPP frequency when compared in amplitude relative to respective humps.

Reduction of Ca^{2+} Entry Does Not Explain the Decline of Ca^{2+}- and MEPP-Humps

Ca^{2+}- and MEPP-humps can be accounted for by several possible mechanisms. First, continuous tetanic stimulation at a high frequency (50 Hz) for several minutes in a low Ca^{2+}, high Mg^{2+} solution may have blocked the conduction of impulses to motor nerve terminals. Second, even if no conduction failure occurred, it might be possible that the increase in $[Ca^{2+}]_i$ induced by con-

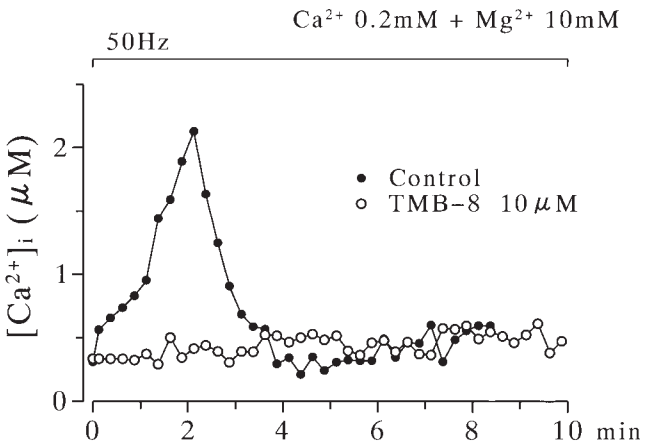

FIGURE 3. Tetanus-induced increases in $[Ca^{2+}]_i$ (Ca^{2+}-hump) and effects of TMB-8. Throughout the data points in graphs, tetanus (50 Hz) was continuously applied. All the recordings were made in a low Ca^{2+} (0.2 mM), high Mg^{2+} (10 mM) solution. Effects of TMB-8 (10 μM) were seen 30 min after treatment with the drug that began after a period of no stimuli for 30 min. Data were obtained from the terminals loaded with Indo-1. Ratios (F_{412}/F_{475}) of fluorescences peaking at 412 (F_{412}) and 475 (F_{475}) nm were converted to $[Ca^{2+}]_i$ values. Experimental protocol is the same as that in Fig. 2 *D*.

tinuous activation of Ca^{2+} entry during a tetanus would cause Ca^{2+}-dependent inactivation of voltage-dependent Ca^{2+} channels (Eckert and Tillotson, 1981; Galli et al., 1994). These mechanisms would have caused the rapid decay of the Ca^{2+}- and MEPP-humps. An experiment to test whether voltage-dependent Ca^{2+} channels are opened by each impulse during tetanus is to apply Mn^{2+} externally and to observe its quenching effects on fluorescent Ca^{2+} probes loaded in the terminals. Mn^{2+} (1.8 mM), applied externally after the end of Ca^{2+}-hump, quickly quenched the fluorescence of Indo-1 at two wavelength ranges (Fig. 4 *A*; $n = 4$) or the fluorescence of Fura-2 measured at 380 nm (Fig. 4 *C*; $n = 1$) (Merritt et al., 1989), indicating the opening of voltage-dependent Ca^{2+} channels by each impulse during this period. On the other hand, Mn^{2+} had little effect on Indo-1 or Fura-2 fluorescence when no stimulation was given to the motor nerve (Fig. 4 *B*, not shown for Indo-1 fluorescence). The results thus indicate that there is neither conduction failure of impulses along motor nerve axons nor the considerable inactivation of Ca^{2+} channels during a continuous tetanus.

Effects of Blockers of Ryanodine Receptors on Ca^{2+}- and MEPP-Humps

The most likely mechanism for Ca^{2+}- and MEPP-humps could be that CICR occurs in response to Ca^{2+} entry and ceases due to depletion of Ca^{2+} stores and/or inactivation of the mechanism. If CICR occurs, it would involve ryanodine receptors rather than inositoltrisphosphate (IP_3) receptors (Bezprozvanny et al., 1991; see also Berridge, 1993), since no agonist of receptors to raise IP_3 level was given under the present experimental condition. Then, if CICR occurs via the activation of ryanodine receptor, its antagonists, TMB-8 (Chiou and Malagodi, 1975) and ryanodine (Sutko et al., 1979) are expected to block Ca^{2+}- and MEPP-humps. This was the case. TMB-8 (4–8 μM) blocked reversibly MEPP-humps, but not later slow progressive rises in MEPP frequency (Fig. 2 *D*; $n = 11$). So did ryanodine (10 μM), but almost irreversibly ($n = 4$; not shown). Likewise, TMB-8 (10 μM; Fig. 3; $n = 3$) and ryanodine ($n = 1$, not shown) completely blocked Ca^{2+}-humps. The results strongly suggest that ryanodine receptors in motor nerve terminals are activated by repetitive Ca^{2+} entries during a continuous tetanus, causing CICR and transiently increasing $[Ca^{2+}]_i$ and MEPP frequency. It might be possible, however, that an increase in $[Ca^{2+}]_i$ by the CICR via ryanodine receptors activates phospholipase C to produce IP_3, which results in further CICR via IP_3 receptors.

It may be noted that TMB-8 (8 μM) decreased the amplitude of MEPP to 81.2 ± 4.8% of the control ($n = 5$; $P < 0.05$; see Hunt et al., 1990). This action, however, did not affect much the above suggestion (see MATERIALS AND METHODS). The possibility that the decline of MEPP-hump results from the depletion of quanta available for release can be ruled out for two reasons. First, the time course of MEPP-hump was similar to that of Ca^{2+}-hump. Second, the MEPP frequency of several hundreds per second is equivalent to the number of quanta released by nerve impulses at 1 or 2 Hz in normal Ringer solution (Gage, 1976), which would cause little depletion of quanta in nerve terminals.

Effects of Inhibitors of Ca^{2+} Uptake at Ca^{2+} Stores

Thapsigargin (1 μM), a blocker of Ca^{2+} pumps at the endoplasmic reticulum membrane, suppressed Ca^{2+}-humps (to 27.4 ± 4.4%, $n = 5$; $P < 0.001$; Fig. 6 *A*) and MEPP-humps (to 45.5 ± 9.8%, $n = 4$; $P < 0.02$; Fig. 6 *B*). These results indicate that thapsigargin-sensitive Ca^{2+} stores are involved in CICR in frog motor nerve terminals. The basal levels of $[Ca^{2+}]_i$ before tetanic stimulation was not significantly changed in the presence of thapsigargin (89.2 ± 18.9 nM, $n = 5$; controls, 69 nM). The $[Ca^{2+}]_i$ values at the end of Ca^{2+}-hump or at the equivalent time in the presence of thapsigargin (131.3 ± 21.9 nM, $n = 5$) were also similar to those of the controls (137.2 ± 33.6 nM, $n = 5$).

Mitochondria are known to retain Ca^{2+} under resting conditions and also to act as Ca^{2+} buffers at a relatively high $[Ca^{2+}]_i$ level in some types of neurones (Duchen et al., 1990; Thayer and Miller, 1990; Friel and Tsien, 1994; Nohmi et al., 1994). It has also been known that

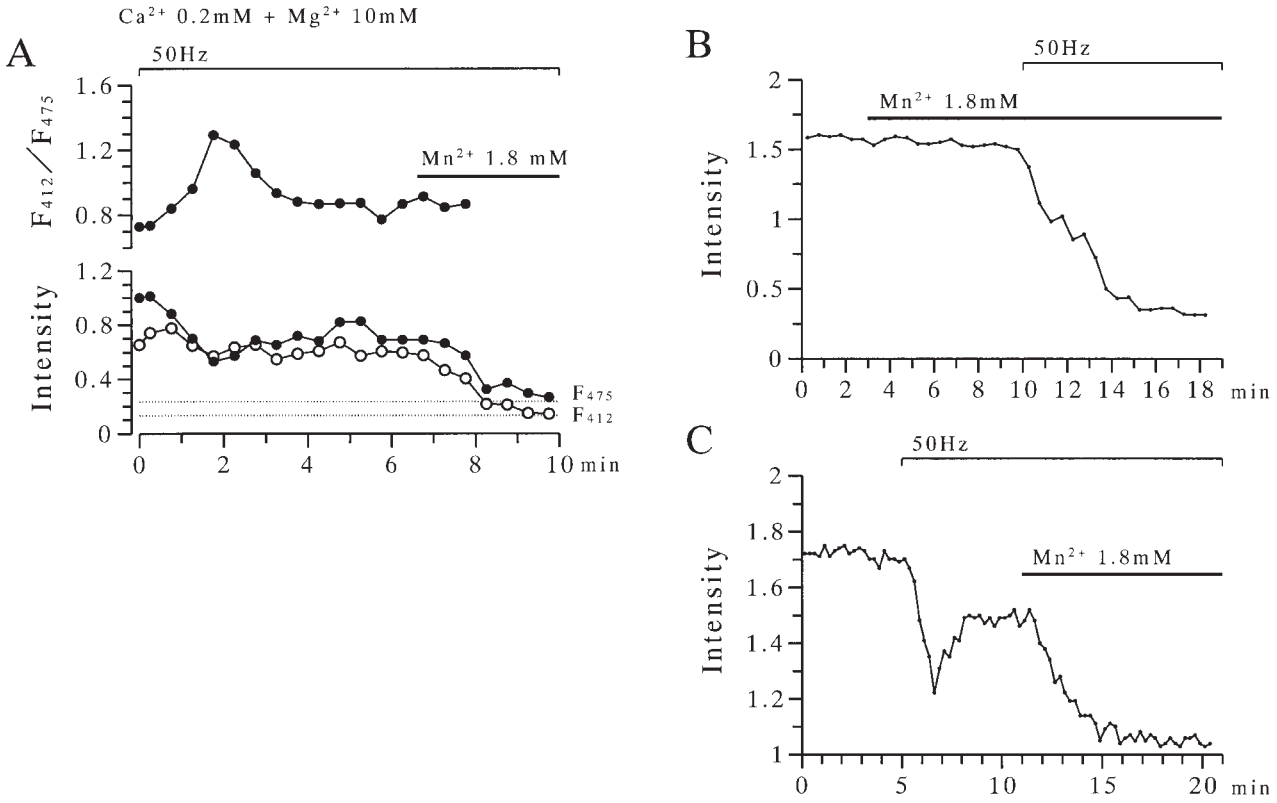

FIGURE 4. Quenching effects of Mn^{2+} on Indo-1 or Fura-2 fluorescence loaded in the terminals. (*A*) Quenching effects of Mn^{2+} on Indo-1 fluorescence. Mn^{2+} (1.8 mM) was applied after the generation of a Ca^{2+}-hump. Note decreases in fluorescence at both wavelength ranges (F_{412} and F_{475}). (The lack of an apparent increase in F_{412} during a rise in F_{412}/F_{475} can be explained by the shift of excitation spectrum of Indo-1 by an increase in $[Ca^{2+}]_i$ to a shorter wavelength range; compare Kuba et al., 1994). (*B*) The lack of quenching effects of Mn^{2+} on Fura-2 fluorescence in the absence of nerve stimuli and the quenching effect during stimuli. Fluorescence was measured at a wavelength range peaked at 380 nm (F_{380}). Fluorescence intensity is shown in an arbitrary unit. (*C*) Quenching effects of Mn^{2+} on Fura-2 fluorescence during tetanic stimuli after the generation of a Ca^{2+}-hump (seen as a transient decrease in fluorescence). Fluorescence was measured at F_{380}.

mitochondria of hepatocytes and heart muscles have a permeability-transition pore, large nonselective ion channel (Bernardi et al., 1993; Szabó and Zoratti, 1993), which is activated by an increase in $[Ca^{2+}]_i$ (Ichas et al., 1997). It might therefore be possible that such large nonselective ion channels may exist in the mitochondria of frog motor nerve terminals and be activated by Ca^{2+} entry. The resultant Ca^{2+} release may have caused Ca^{2+}-humps. Application of a mitochondrial poison, CN^- (2 mM), to frog motor nerve terminals increased the basal level of $[Ca^{2+}]_i$ from 69 to 93.2 ± 4.1 nM ($n = 4$; $P < 0.2$). Although the difference was not statistically significant, this may suggest that the mitochondria in frog terminals indeed retain Ca^{2+} in a certain amount. The poison, however, did not block the Ca^{2+}-hump, but instead enhanced it (to 557.0 ± 119.3% of the control in CN^-, $n = 3$; $P < 0.05$; Fig. 6 *C*). Furthermore, the basal $[Ca^{2+}]_i$ at the end of Ca^{2+}-hump was significantly increased from 99.2 ± 25.7 to 152.1 ± 15.7 nM ($n = 4$; $P < 0.1$) in the presence of CN^-. Thus, it is obvious that mitochondria are not involved in CICR in motor nerve terminals, but in the buffering of the resultant rise in $[Ca^{2+}]_i$.

The Time Course of the Activation of CICR

The component of CICR in the time course of a Ca^{2+}- or MEPP-hump may be demonstrated in three ways. First, it can obviously be shown by a difference between the time courses of $[Ca^{2+}]_i$ during a tetanus in the absence and presence of TMB-8 and also by a difference between those of MEPP frequency (see Figs. 2 *D* and 3). There were similarities between the time courses of the TMB-8-sensitive components of Ca^{2+}-and MEPP-humps. The second method to estimate the time course of CICR activation would be to stop Ca^{2+} entry, and so the activation of CICR, by a short pause (5 s) in tetanus and to measure the magnitude of resultant reductions in $[Ca^{2+}]_i$ or MEPP frequency. Pauses during a MEPP-hump quickly reduced MEPP frequency to a low level (Fig. 7 *A*), equivalent to that solely caused by Ca^{2+} entry under the blockade of CICR by TMB-8 (Fig. 2 *D*). Thus, the mag-

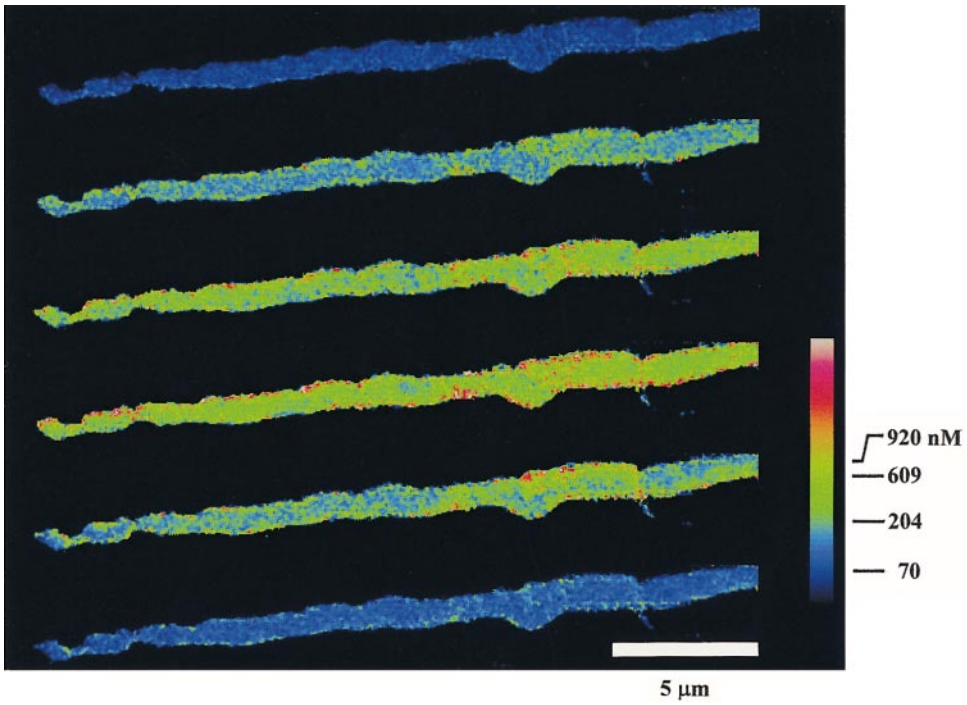

FIGURE 5. Tetanus-induced increases in the fluorescence of Oregon Green BAPTA-1 in the motor nerve terminals. 50 Hz tetanus was given to the nerve throughout the experiments. All the images are shown by the ratio to that before tetanus. The image in the top is the control, which is the ratio of an image to another before the beginning of stimulation. The second to sixth images are those taken at 1, 2, 3, 4, and 5 min after the beginning of tetanus. The ratio values averaged over each image are used in the initial part of the graph in Fig. 10 *A*.

nitude of net reduction in MEPP frequency produced by a pause slowly increased up to a time at the peak of MEPP-hump, and then declined to zero after the end of MEPP-hump so that MEPP frequency was little changed during a short pause after the disappearance of the TMB-8-sensitive component. The time course of the magnitude of pause-induced decrease in MEPP frequency resembled that of the TMB-8-sensitive component of MEPP-hump. The third method to estimate the time course of changes in the rate of Ca^{2+} release during the course of tetanus could be to measure alterations in the initial rate of rise in MEPP frequency after a pause (see MATERIALS AND METHODS). They increased during the rising phase of a MEPP-hump and decreased during the falling phase to a moderate level, which remained constant as long as tetanus continued (Fig. 7 *B*). (The reason for the incomplete reduction of the initial rate of rise to that at the beginning of tetanus was found to be due to recovery from inactivation of the Ca^{2+} release mechanism during a pause; see below.) Thus, CICR begins to be slowly activated over minutes and subsides at the rate faster than the growth of its activation. Furthermore, the appearance of the component of CICR at the initial phase of tetanic stimulation indicates that Ca^{2+} stores in frog motor nerve terminals are normally filled with Ca^{2+} in an amount at least enough for release in response to Ca^{2+} entry (see DISCUSSION for details).

Ca^{2+} Entry-dependent Inactivation of the CICR Mechanism

Another important effect of applying pause in tetanus during the falling phase of MEPP-hump is a rebound increase in MEPP frequency after the pause to a value greater than the level of the hump (Fig. 7 *A*). Furthermore, resuming tetanus after a pause given in a period after MEPP-hump induced a quick increase in MEPP frequency, although there was little change in MEPP frequency during the pause (Figs. 7 *A* and 8 *A*). These post-pause increases in MEPP frequency were blocked by TMB-8 (8 μM; $n = 3$; Fig. 8 *B*) and thapsigargin (1 μM; to 21 and 19%, $n = 2$; Fig. 6 *B*). Likewise, a sharp rise in $[Ca^{2+}]_i$ occurred after a pause in tetanus given after the end of a Ca^{2+}-hump, although there was a negligible change during the pause (Figs. 9 and 10 *A*). This post-pause rise in $[Ca^{2+}]_i$ was blocked by ryanodine (not shown; 10 μM; $n = 1$). Thus, the post-pause increases in MEPP frequency and $[Ca^{2+}]_i$ must be caused by the reactivation of CICR. In addition, the fact that stopping tetanus at a time after the end of MEPP- or Ca^{2+}-hump had little effect on MEPP frequency and $[Ca^{2+}]_i$ level strongly indicates that CICR is inactivated under this condition. Then, the quick increases in $[Ca^{2+}]_i$ and MEPP frequency after the resumption of tetanus suggest that the inactivation of the CICR mechanism is removed during the pause. If so, the extent of recovery from inactivation should depend on the duration of pause. This was indeed the case. The magnitude of the post-pause rise in MEPP frequency was increased, as pause duration was made longer (Figs. 8 *A* and 10 *B*). Likewise, the magnitude of post-pause rise in $[Ca^{2+}]_i$ was augmented, as pause duration was increased (Figs. 9 and 10, *A* and *B*). The results suggest that the recovery of Ca^{2+} entry-dependent inactivation of CICR occurs rather quickly over several tens of seconds. The possibility that

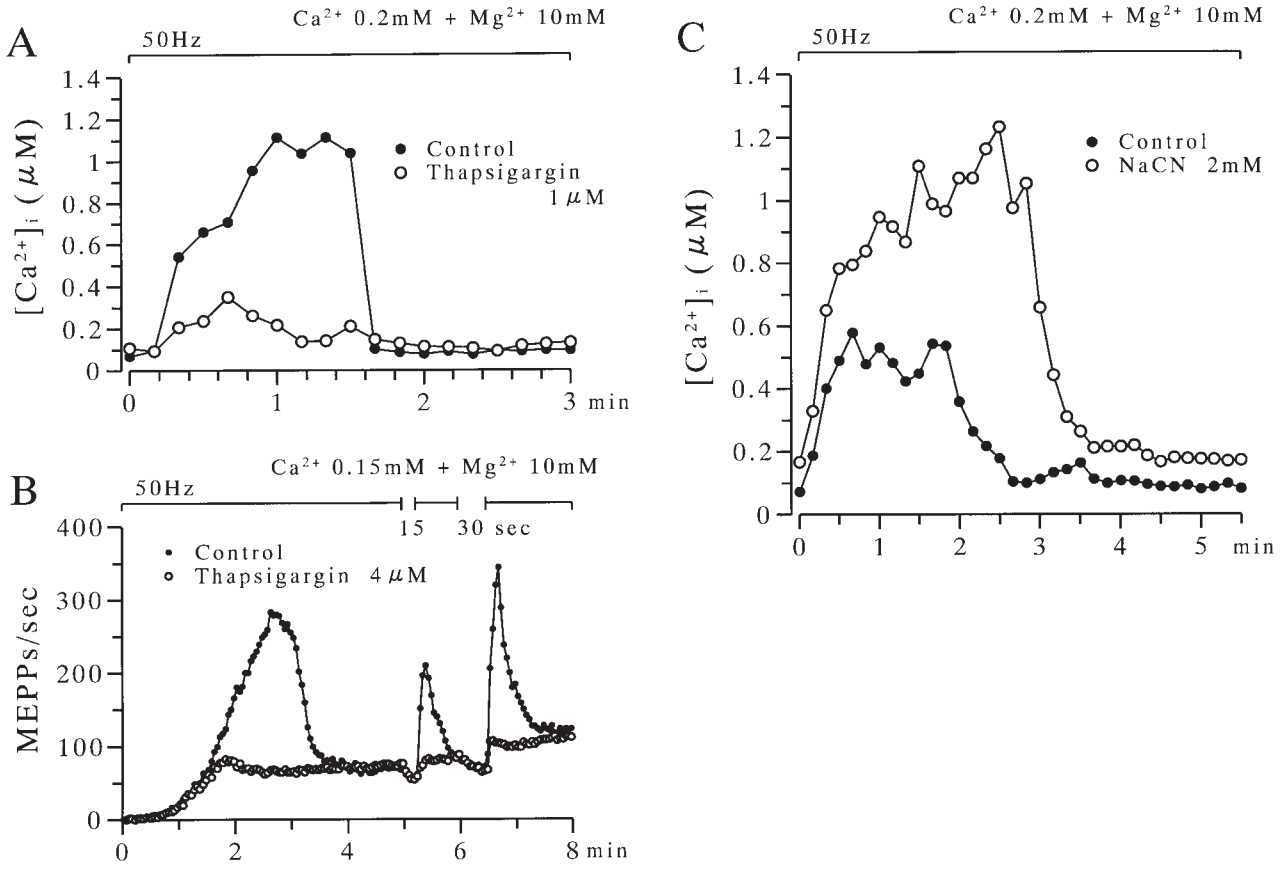

FIGURE 6. Effects of thapsigargin and CN^- on Ca^{2+}-humps and effects of thapsigargin on MEPP-hump during continuous tetanic stimulation in a low Ca^{2+}, high Mg^{2+} solution. (*A*) Effects of thapsigargin on a Ca^{2+}-hump. 50 Hz tetanus was given to the nerve in the absence or presence of thapsigargin (1 μM). After recording the control, the preparation was left without stimuli for 30 min in a low Ca^{2+}, high Mg^{2+} solution, and then superfused with a drug-containing solution for a period of 30 min before the beginning of stimulation. (*B*) Effects of thapsigargin (4 μM) on a MEPP-hump and post-pause rises in MEPP frequency. The time interval between the measurements of MEPPs in the absence and presence of the drug and the duration of drug application are the same as those in *A*. (*C*) Effects of CN^- (2 mM). 50 Hz tetanus was given to the nerve in the absence or presence of CN^-. After taking the control, the preparation was left for 30 min without stimuli in a low Ca^{2+}, high Mg^{2+} solution and subsequently superfused with a CN^--containing solution for 9 min before the beginning of stimulation.

the dependence of post-pause rises in $[Ca^{2+}]_i$ and MEPP frequency on pause duration reflects a process of Ca^{2+} uptake into Ca^{2+} stores can be ruled out by the lack of a reduction in $[Ca^{2+}]_i$ or MEPP frequency during a pause (see DISCUSSION).

Ca^{2+} Entry-dependent Priming and Depriming of the CICR Mechanism

A gradual increase in the rate of Ca^{2+} release during tetanus, as shown in Figs. 2 *B*, 3, and 7, *A* and *B*, suggests that the mechanism of CICR slowly changes into an activable state in response to tetanus. This process may be called "priming." The dependence of the slow onsets of MEPP (Fig. 2 *B*) and Ca^{2+}-humps on $[Ca^{2+}]_o$ suggests the role of Ca^{2+} entry in the mechanism of priming. Fig. 11 shows an experiment to test this possibility. A 50-Hz tetanus was given for 7 min in a Ca^{2+}-free (1 mM EGTA), Mg^{2+} (1 mM) solution, and then a low Ca^{2+} (0.2 mM), high Mg^{2+} (10 mM) solution was superfused for 5 min without applying tetanus. Resumption of tetanus after this "conditioning treatment" caused only a small and slow increase in MEPP frequency (Fig. 11, *A a* and *B a*). This small increase by 50 Hz tetanus may presumably be due to depletion of Ca^{2+} in Ca^{2+} stores. On the other hand, after a 50-Hz tetanus for 7 min with the subsequent pause for 5 min in the low Ca^{2+}, high Mg^{2+} solution, MEPP frequency was sharply increased in response to the resumption of tetanus (Fig. 11 *Ab, Ad, Bb,* and *Bd*). Thus, Ca^{2+} entry during "the conditioning tetanus" is necessary for priming the mechanism of CICR in frog motor nerve terminals.

When tetanus was stopped for a sufficiently long period, 79 min, after the end of a MEPP-hump, the subse-

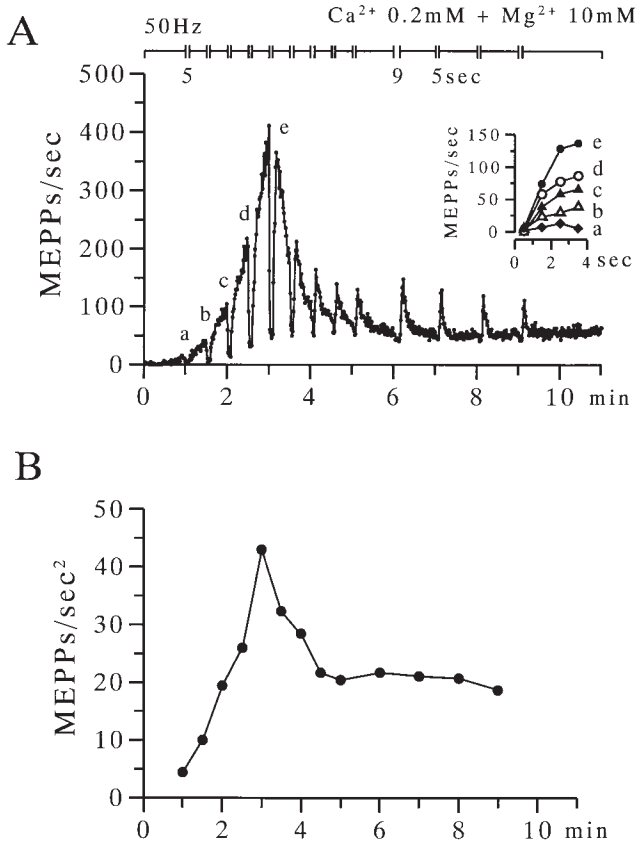

FIGURE 7. The time course of CICR activation: effects of brief pauses in tetanus on MEPP frequency during and after a MEPP-hump. (*A*) Changes in MEPP frequency caused by a pause in tetanus (50 Hz) applied during and after a MEPP-hump. Pauses of 5 or 9 s were applied during a period indicated by a horizontal bar. Inset is the expansions of the rising phases of MEPP frequency after a short pause (5 s) given at 1 (*a*), 1.5 (*b*), 2 (*c*), 2.5 (*d*), and 3 (*e*) min after the beginning of a tetanus (50 Hz). Abscissa is the time after resumption of tetanus, while ordinate represents a net increase in MEPP frequency. (*B*) Changes in the initial rate of rise of MEPP frequency after a pause during the course of a series of tetani (50 Hz). The rate of rise of MEPP frequency was measured from the slope of the regression line fitted to the initial three data points. Note that the time for the peak of the rate of rise roughly corresponds to the peak of MEPP-hump.

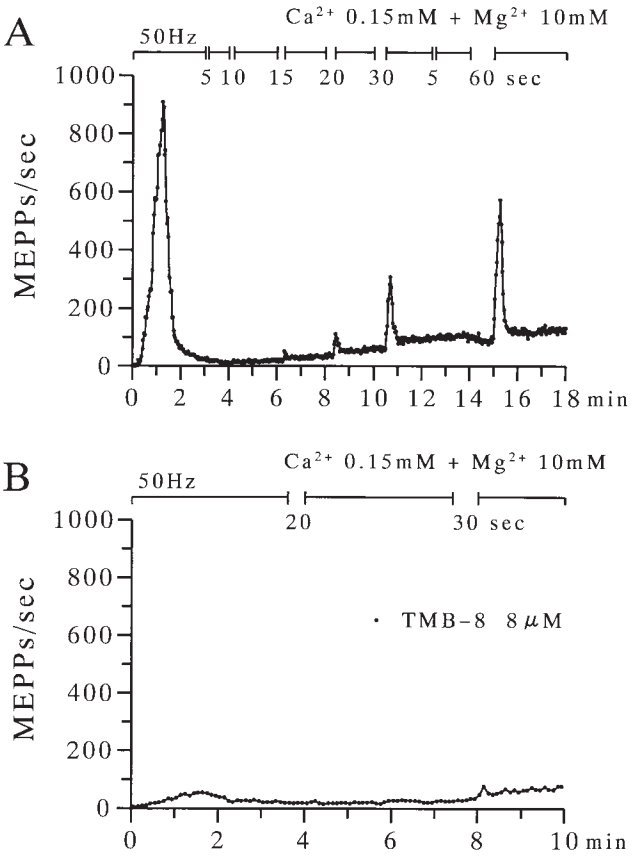

FIGURE 8. The dependence of post-pause increases in MEPP frequency on pause duration and effects of TMB-8. (*A*) Rises in MEPP frequency after brief pauses of different duration in tetanus (50 Hz) applied after a MEPP-hump. (*B*) Effects of TMB-8 (8 μM) on MEPP-hump and post-pause rises in MEPP frequency. Experimental protocol is the same as that in Fig. 2 *D*.

quent resumption of tetanus produced an increase in MEPP frequency (Fig. 11 *Ac*) whose rate was similar to that of MEPP-hump (Fig. 2 *D*). Accordingly, the absence of nerve activity would decrease the readiness for activation of the CICR mechanism. This process may be defined as the depriming of the CICR mechanism. The time course of depriming can be estimated by giving longer pauses of variable duration (1–60 min) after a MEPP-hump. As pause duration was increased, the time course of post-pause rise in MEPP frequency became slower, resembling that of the initial MEPP-hump (Fig. 12 *A*). The initial rate of post-pause rise to 10% of the maximum amplitude, reflecting the rate of Ca^{2+} release, slowly decreased over tens of minutes (Fig. 12 *B*).

DISCUSSION

The present study demonstrates the slow, transient activation of CICR in response to repetitive Ca^{2+} entries in frog motor nerve terminals. Continuous tetanic nerve stimulation (20–50 Hz) produced slow transient increases in $[Ca^{2+}]_i$ in the motor nerve terminals and MEPP frequency in a low Ca^{2+}, high Mg^{2+} solution, which were reduced in amplitude by lowering $[Ca^{2+}]_o$ and decreasing stimulation frequency and blocked by antagonists of ryanodine receptors, TMB-8, and ryanodine, and an antagonist of intracellular Ca^{2+} pump, thapsigargin. Further analyses of the mode of CICR activation revealed the unique Ca^{2+} entry-dependent priming, depriming, inactivation, and deinactivation of the CICR mechanism.

The evidence for this conclusion was obtained by independent measurements of MEPP frequency and $[Ca^{2+}]_i$ in the motor nerve terminals from different muscle preparations. Accordingly, relevancy and limitations for the use of different muscles must be stated be-

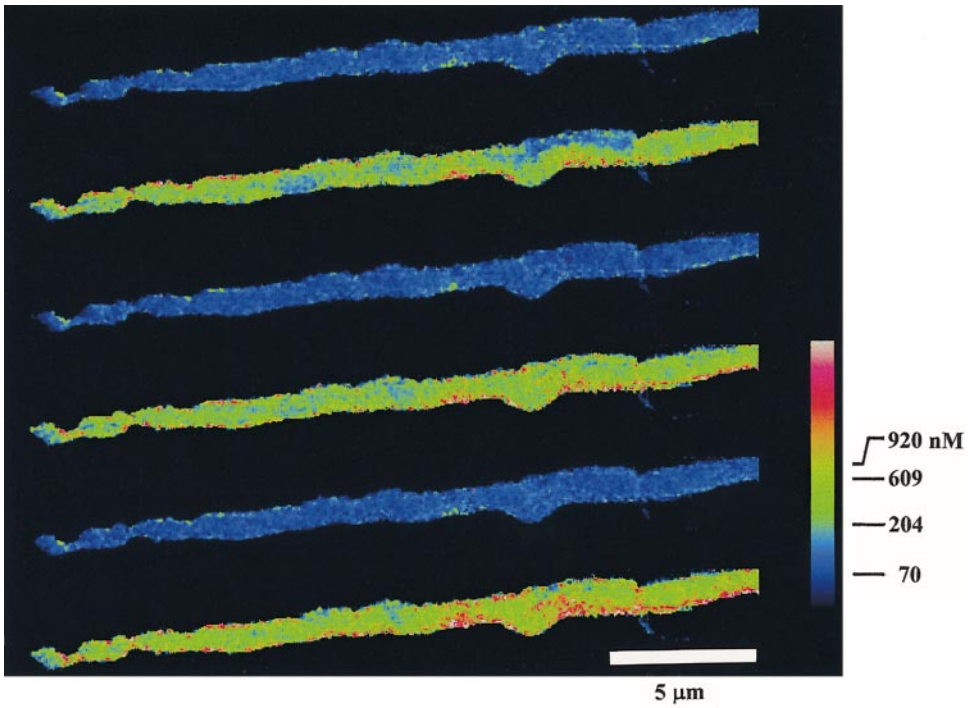

FIGURE 9. Increases in the fluorescence of Oregon Green BAPTA-1 in the motor nerve terminals after pauses of different duration during a 50-Hz tetanus. All the images are shown in ratios of fluorescence to that before the beginning of tetanus. The first, third, and fifth images from the top were taken at the end of each pause, while the second, fourth, and sixth images were taken at the peak of increases after pauses of 10, 30, and 60 s. The images were taken immediately after recording the images shown in Fig. 5 from the same cell. The ratio values averaged over each image fulfilled the data points in the later part of the graph in Fig. 10 *A*.

fore discussing the evidence and rationale leading to the proposition of the unique mechanisms of CICR in frog motor nerve terminals. First, both the sartorius and cutaneous pectoris muscles of frogs are of fast type. Each muscle fiber is innervated by a single or a few nerve(s) and the nerve terminals are those of an elongated shape (Birks et al., 1960; Peper and Dreyer, 1974). Second, changes in $[Ca^{2+}]_i$ and MEPP frequency in response to tetanus and its interruption are quite similar. Third, the modes of actions of drugs that affect Ca^{2+} release and uptake are essentially identical. An apparent limitation in the interpretation of the data obtained from different preparations would be that changes in $[Ca^{2+}]_i$ cannot be directly correlated to those in MEPP frequency.

There are at least three factors that decide the magnitude of CICR from Ca^{2+} stores; the amount of trigger Ca^{2+}, the rate constant of Ca^{2+} release (γ in Eq. 1 or 2), and the amount of Ca^{2+} in Ca^{2+} stores.

Experimental Parameters Reflecting the Rate of Ca^{2+} Release

It may be safe to assume that the amount of Ca^{2+} influx accompanying each impulse during tetanus does not change to an extent affecting the activation of CICR for two reasons. First, there was only a small change in the level of $[Ca^{2+}]_i$ increased only by Ca^{2+} entry during the course of continuous tetanus under the blockade of CICR (Figs. 3 and 6 *A*). Second, Mn^{2+} applied externally quenched Indo-1 or Fura-2 fluorescence after the generation of Ca^{2+}-hump (Fig. 4, *A* and *C*), indicating the opening of voltage-dependent Ca^{2+} channels throughout the course of tetanic stimulation. Accordingly, Eq. 2, expressing the rate of Ca^{2+} release, can be reduced to

$$\gamma z \approx (1 + \kappa_s)\, dx/dt + (\alpha + p)\, x. \qquad (5)$$

Thus, changes in the rate of Ca^{2+} release can be predominantly reflected in either or both of two experimental variables: the levels of the $[Ca^{2+}]_i$ (x) or MEPP frequency (the power function of x) via constants ($\alpha + p$) and the initial rate of rise in $[Ca^{2+}]_i$ (dx/dt) or MEPP frequency via constants, ($1 + \kappa_s$). When dx/dt is slow, enough for the steady/equilibrium approximation, the rate of Ca^{2+} release could be represented predominantly by the level of $[Ca^{2+}]_i$ or MEPP frequency, as shown in Eq. 3. On the other hand, when the initial rate of post-pause rise is measured from a relatively low and constant level, it would also reflect the rate of Ca^{2+} release, as shown in Eq. 4. Relevancy of applying these ideas (see also MATERIALS AND METHODS) to the present experimental data was tested.

The rate of changes in $[Ca^{2+}]_i$ at the half maximum point of the rising phase of a Ca^{2+}-hump was 10 nM/s (Fig. 3), yielding 4.5 μM/s for $(1 + \kappa_s)\, dx/dt$ in Eq. 5, assuming 450 (90×5) of κ_s (90 for Ca^{2+} binding proteins taken from measurements by Neher and Augustine, 1992; mitochondrial factor was assumed to be 5 based on the effect of CN^- on Ca^{2+}-hump). The rate constant for Ca^{2+} removal ($\alpha + p$) from frog motor nerve terminals can be estimated from the rate of a rise in $[Ca^{2+}]_i$ to a plateau in response to a short tetanus in normal Ringer. A rise in $[Ca^{2+}]_i$ produced by 50 Hz in normal Ringer solution reached a plateau in 0.2 s (our

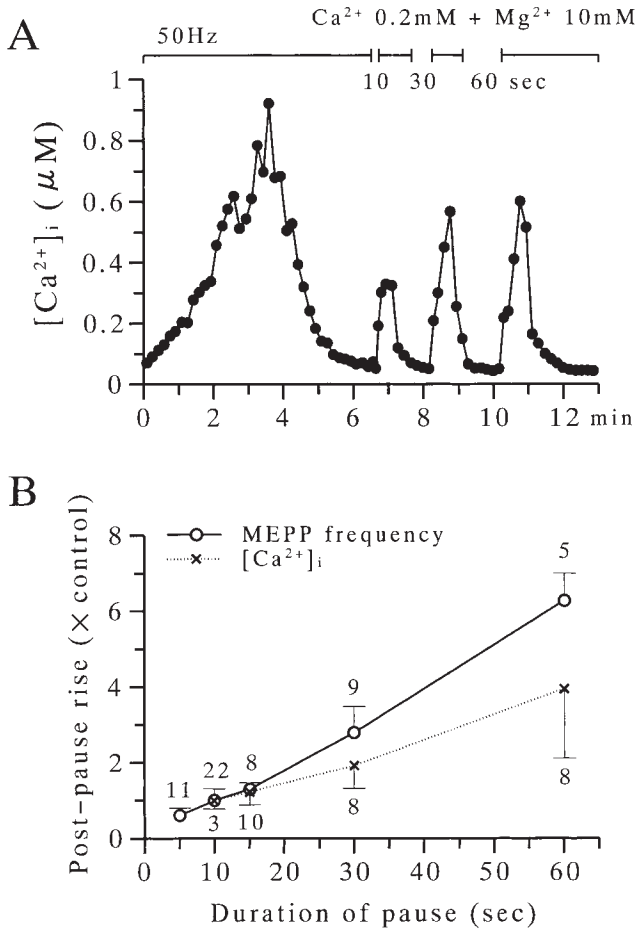

FIGURE 10. The dependence of post-pause rises in $[Ca^{2+}]_i$ and MEPP frequency on pause duration. (*A*) Ca^{2+}-hump and increases in $[Ca^{2+}]_i$ after brief pause in tetanus (50 Hz). The data points were plotted from the experiments shown in Figs. 5 and 9. (*B*) Relationships between the magnitude of post-pause rise in MEPP frequency or $[Ca^{2+}]_i$ and the duration of pause. (○) MEPP frequency; (×) $[Ca^{2+}]_i$. Each data point is the average of those obtained from different terminals, whose number is shown above or below each point. The magnitudes of post-pause rises in MEPP frequency and $[Ca^{2+}]_i$ for each duration of pause were normalized to those at 10 s pause, and then their average and SEM were taken. MEPPs were recorded from frog sartorius muscles, while changes in $[Ca^{2+}]_i$ were from motor nerve terminals of frog cutaneous pectoris muscles.

unpublished observations). Solving Eq. 1 for $\gamma = 0$ (since Ca^{2+} release channels would not be primed for a short period of 0.2 s), the time constant (0.2 s) to reach the plateau is $(1 + \kappa_s)/(\alpha + p)$, yielding a value of 2,255 s^{-1} [= (1 + 450)/0.2] for $(\alpha + p)$. Then, taking a value of 1.4 μM at the midpoint of the rising phase of Ca^{2+}-hump, $(\alpha + p)x$ during the course of a Ca^{2+}-hump would be 3,157 μM/s (= 2,255 s^{-1} × 1.4 μM). Thus, $(\alpha + p)x$ is greater than $(1 + \kappa_s)dx/dt$ (= 4.5 μM/s) during the rising phase of Ca^{2+}-hump. Accordingly, $(\alpha + p)x$ is the major determinant factor for γz, the rate of Ca^{2+} release, in Eq. 5, indicating that the level of $[Ca^{2+}]_i$ (and also MEPP frequency) itself reflects the rate of Ca^{2+} release (Eq. 3).

When the initial rates of post-pause rise in $[Ca^{2+}]_i$ (dx/dt in Eq. 5) were compared at similar low values of $[Ca^{2+}]_i$ during the course of Ca^{2+}-hump, it would also represent the rate of Ca^{2+} release. This idea may be supported by a relatively small value of $(\alpha + p)x$ at the end of each pause, from which the initial rate of post-pause rise was measured. When the level of $[Ca^{2+}]_i$ is as low as a few hundred nanomolars, the time constant of Ca^{2+} removal is slow and in the order of seconds (our unpublished observations), say 5 s, yielding a value of 90.2 s^{-1} [= (1 + 450)/5] for $(\alpha + p)$. Then, $(\alpha + p)x$ during a pause in tetanus, during which $[Ca^{2+}]_i$ was 0.15 μM, would be 13.5 μM/s (= 90.2 × 0.15 μM/s). This is still larger than $(1 + \kappa_s)dx/dt$ measured from a post-pause rise in $[Ca^{2+}]_i$ after a Ca^{2+} hump [say 6.8 μM/s (15 nM/s × 451) from the data shown in Fig. 10 *A*] and presumably also that during Ca^{2+}-hump, although it was not measured in the present study. Nevertheless, when the rates of Ca^{2+} release are compared at similar values of $[Ca^{2+}]_i$, their changes may be safely represented by changes in the initial rate of post-pause rise. In support of this, the time course of changes in the initial rate of post-pause rise in MEPP frequency reflecting changes in $[Ca^{2+}]_i$ during the course of a MEPP-hump paralleled that of the hump itself (Fig. 7, *A* and *B*).

Priming, Depriming, Inactivation, Deinactivation of the Ca^{2+} Release Mechanism

The rate of Ca^{2+} release (γz in Eq. 5) is the product of rate constant (γ) for Ca^{2+} release (the number and open probability of Ca^{2+} release channels) and $[Ca^{2+}]_s$ (z). The rate of Ca^{2+} release, reflected at the level of MEPP frequency or $[Ca^{2+}]_i$ or the initial rate of post-pause rise in MEPP frequency during MEPP- or Ca^{2+}-hump, increased during the rising phase of the humps. In contrast, $[Ca^{2+}]_s$ should have decreased during this phase (see the next section). Consequently, the rate constant for Ca^{2+} release (γ) must have increased during the rising phase of Ca^{2+}- or MEPP-hump. This slow rise in rate constant for Ca^{2+} release, called the priming of the CICR mechanism, could be due to an increase in the readiness for activation or in open probability or number of Ca^{2+} release channels. The priming process was found to be dependent on Ca^{2+} entry, as seen in the dependence of MEPP-hump on $[Ca^{2+}]_o$ (Fig. 2 *B*) and the lack of priming effect of tetanus in a Ca^{2+}-free solution to produce a quick rise in MEPP frequency like a post-pause rise (Fig. 11 *A a*).

Based on the rationale discussed above, the rate of Ca^{2+} release decreased during the falling phase of Ca^{2+}- and MEPP-humps and became zero after the end

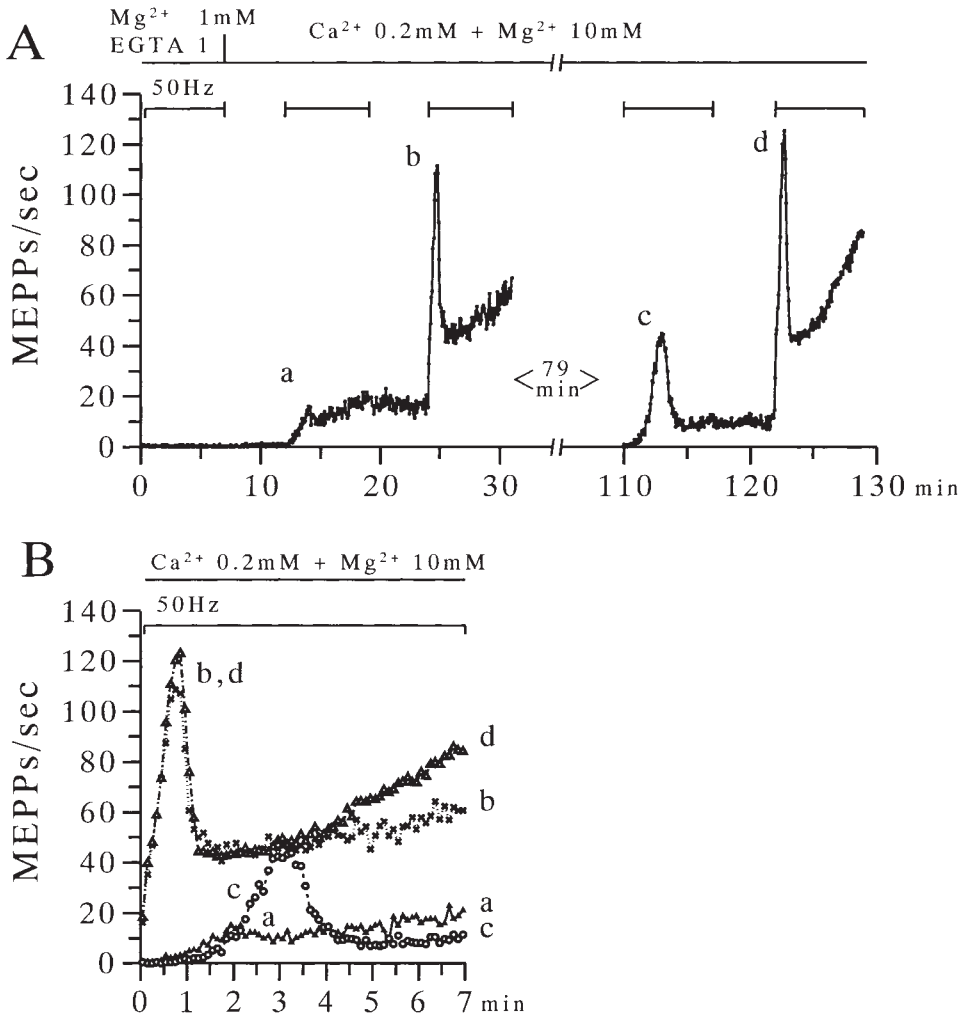

FIGURE 11. Ca^{2+} dependence of the priming effect of tetanus. (*A*) The lack of the facilitatory effect of a tetanus (the first of horizontal bars) in a Ca^{2+} free (1 mM EGTA), Mg^{2+}(1 mM) solution on the induction of MEPP-hump. After tetanus (50 Hz) was given for ~7 min in a Ca^{2+} free (1 mM EGTA), Mg^{2+} (1 mM) solution, the preparation was superfused with a low Ca^{2+} (0.2 mM), high Mg^{2+} (10 mM) solution for 5 min. This was followed by several tetani (50 Hz; horizontal bars) of 7 min at an interval of 5 or 79 min. (*B*) Transient rises in MEPP frequency after resumption of tetanus (*a, b, c, d*) replotted in the expanded time scale. Abscissa represents the time after resumption of tetanus.

of humps. This is also supported in part by the decrease in the initial rate of post-pause rise in MEPP frequency during the decay phase of MEPP-hump (Fig. 7 *B*), although it did not decrease to zero because of the effects of pause on the readiness for the activation of Ca^{2+} release (see below). The slow decrease in the rate of Ca^{2+} release to zero may be caused by depletion of Ca^{2+} in stores, the reversal of priming process, or the inactivation of Ca^{2+} release channels. The generation of post-pause rises in $[Ca^{2+}]_i$ or MEPP frequency after the end of Ca^{2+}- or MEPP-hump indicates that Ca^{2+} stores involved in CICR are filled with Ca^{2+} in a considerable amount for release under this condition (see below). Furthermore, the fact that the rate of the post-pause rises in $[Ca^{2+}]_i$ and MEPP frequency immediately after the end of Ca^{2+}- and MEPP-hump, respectively, was much faster than the rate of rise of each hump suggests that the decay phase of Ca^{2+}- and MEPP-humps cannot be explained by the depriming of the CICR mechanism. (If it were so, the rate of post-pause rise must have been as slow as that of humps.) Accordingly, the CICR mechanism would lie in another state after the end of Ca^{2+}- and MEPP-humps, which is inactivation produced by Ca^{2+} entry. Then, the increase in the amplitude of post-pause rise in MEPP frequency or $[Ca^{2+}]_i$ with an increase in pause duration would therefore represent the rate of recovery from Ca^{2+}-dependent inactivation. Ca^{2+}-dependent inactivation of Ca^{2+} release channels in neurones was recently suggested by Hernandez-Cruz et al. (1997). The fact that a short pause changed little the level of $[Ca^{2+}]_i$ during it, but produced a sharp rise in $[Ca^{2+}]_i$ after the pause, suggests that Ca^{2+} entry itself or the high $[Ca^{2+}]_i$ close to the intracellular orifice of voltage-dependent Ca^{2+} channels at the cell membrane may inactivate Ca^{2+} release channels, while the absence of Ca^{2+} entry results in recovery from inactivation in frog motor nerve terminals.

On the other hand, a longer pause (>1 min) decreased the rate of post-pause rise in MEPP frequency to that of MEPP-hump produced by the initial application of tetanus. Thus, this slow dependence of the rate

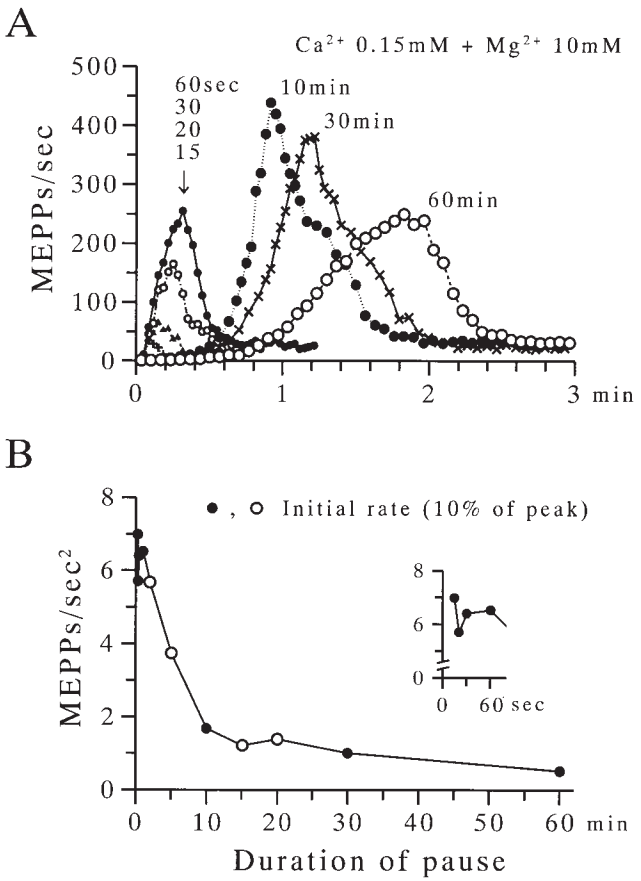

FIGURE 12. Evidence for depriming process: effects of long pauses in tetanus on MEPP frequency after a MEPP-hump. (*A*) Rises in MEPP frequency produced by the resumption of tetanus (50 Hz) after pauses of different duration. Time scale in abscissa represents the time after resumption of tetanus. (*B*) The relationship between the initial rate of post-pause rise in MEPP frequency and the duration of pause. The initial rate of rise was defined as the rate of rise from the MEPP frequency at the beginning of a resumed tetanus to 10% of the peak. (○ and ●) The data points obtained from two different end-plates. The data points shown by open circles were normalized to that shown by the closed circle at 1 min, and then rescaled to values in MEPPs/s^2. (*inset*) The expansion of the initial part of the graph on a faster time scale.

of post-pause rise in MEPP frequency on pause duration would indicate the depriming process of CICR.

The tentative mechanisms of priming, activation, inactivation, and depriming of ryanodine receptor/Ca^{2+} release channels in frog motor nerve terminals may be summarized as follows. Ryanodine receptor/Ca^{2+} release channels are slowly primed in response to repetitive Ca^{2+} entries. Once Ca^{2+} release channels are primed, they are swiftly activated by subsequent Ca^{2+} entry. Further continuation of Ca^{2+} entry inactivates the Ca^{2+} release channels so that inactivation occurs after priming and/or activation. The Ca^{2+} entry-dependent inactivation is quickly removed by stopping Ca^{2+} entry for a short period (<1 min). A longer cessation (>1 min) of Ca^{2+} entry resulted in the depriming of Ca^{2+} release channels over tens of minutes.

Changes in the State of Ca^{2+} Stores Involved in CICR

Changes in the state of Ca^{2+} stores before and during tetanic stimulation may be estimated from the time course of the TMB-8-sensitive component of MEPP- or Ca^{2+}-hump based on the model in Fig. 1. Since the amount of Ca^{2+} influx by each nerve impulse is negligible compared with that of Ca^{2+} release throughout most of Ca^{2+}-hump, the rate of changes in $[Ca^{2+}]_i$ (dx/dt) in the TMB-8-sensitive component of Ca^{2+}- and MEPP-hump must be reflected in changes in the rates of Ca^{2+} release, uptake, and extrusion as shown in the equation:

$$(1 + \kappa_s)\, dx/dt \approx \gamma z - (\alpha + p)\, x. \qquad (6)$$

During the rising phase of TMB-8-sensitive component of Ca^{2+}- or MEPP-hump ($dx/dt > 0$), the rate of Ca^{2+} release (γz) must be greater than the sum of the rates of Ca^{2+} extrusion and uptake $[(\alpha + p)x]$, indicating a progressive decrease in the amount of Ca^{2+} stores during the rising phase of Ca^{2+}- or MEPP-hump. Furthermore, the fact that the TMB-8-sensitive component of a rise in $[Ca^{2+}]_i$ or MEPP frequency occurred without a delay after the beginning of tetanus (see Figs. 2 *D* and 3) suggests that CICR takes place from the beginning of tetanus. This implies that Ca^{2+} stores must be normally filled with Ca^{2+} before the beginning of tetanus.

During the falling phase of MEPP- or Ca^{2+}-hump ($dx/dt < 0$), the sum of the rates of Ca^{2+} uptake and extrusion $[(\alpha + p)x]$ must be greater than the rate of Ca^{2+} release (γz). Although it is not known how much Ca^{2+} is taken up into Ca^{2+} stores after the end of Ca^{2+}- or MEPP-hump, there is evidence to suggest the extent of filling of Ca^{2+} stores after the end of Ca^{2+}- or MEPP-hump. A short pause applied immediately after the humps, which affected little $[Ca^{2+}]_i$ or MEPP frequency during it, produced a sharp and significant increase in $[Ca^{2+}]_i$ or MEPP frequency after the pause. These post-pause rises in $[Ca^{2+}]_i$ and MEPP frequency were blocked by TMB-8 or thapsigargin, indicating that they are induced by CICR from the Ca^{2+} stores that are involved in the generation of Ca^{2+}- and MEPP-humps. If Ca^{2+} stores were to be depleted of Ca^{2+} after the end of Ca^{2+}- or MEPP-hump, Ca^{2+} must have been taken up into Ca^{2+} stores during the pause to produce such a CICR. This should have caused a marked reduction in $[Ca^{2+}]_i$ during the pause, which is equivalent in time integration to the post-pause rises in $[Ca^{2+}]_i$. Thus, it is likely that a considerable amount of Ca^{2+} remains in Ca^{2+} stores after the end of Ca^{2+}- or MEPP-hump. This could be due to a large amount of Ca^{2+} stored in Ca^{2+} stores under the resting condition or to an effective Ca^{2+} uptake during the decay phase of Ca^{2+}- or MEPP-

hump. Such a Ca^{2+} uptake may be achieved by the Ca^{2+} pump, which is activated by the Ca^{2+} in high $[Ca^{2+}]_i$ domains produced around the site of Ca^{2+} release, as suggested for Ca^{2+} stores in bullfrog sympathetic ganglion cells (Cseresnyé et al., 1997).

Comparison with CICRs in Other Neurones

The mode of activation of CICR in frog motor nerve terminals may be compared with those of other neurones in several respects. First, the Ca^{2+} stores in frog motor nerve terminals are normally filled with Ca^{2+} under the resting condition. This characteristic resembles that of Ca^{2+} stores in bullfrog sympathetic ganglion cells (Kuba and Nishi, 1976; Hua et al., 1993), but differs from those in rat sensory neurones (Usachev et al., 1993) and bullfrog sympathetic preganglionic COOH terminals (Peng, 1996). Secondly, the graded activation of CICR in frog motor nerve terminals is similar to those in bullfrog sympathetic ganglion cells (Hua et al., 1993) and rat cerebellar neurones (Llano et al., 1994), but different from the full activation of CICR by Ca^{2+} entry accompanying a single action potential in rabbit otic ganglion cells (Yoshizaki et al., 1995). Thirdly, Ca^{2+}-dependent inactivation of the CICR mechanism in frog motor nerve terminals is similar to that suggested for mammalian sympathetic neurones (Hernandez-Cruz et al., 1997), but differs in the mode of Ca^{2+} dependence. In frog motor nerve terminals, Ca^{2+} release channels appeared to be inactivated by Ca^{2+} entry, not the $[Ca^{2+}]_i$ in the bulk phase, while in mammalian sympathetic ganglion cells CICR seems to be inactivated by the rise in $[Ca^{2+}]_i$ produced by Ca^{2+} release. Finally, the most unique characteristics of CICR in frog motor nerve terminals, which are slow priming and depriming mechanisms, are not seen, to our knowledge, in other types of neurones or in muscles. Thus, these properties in frog motor nerve terminals are quite different from those in other cells.

The Physiological Significance of CICR in the Presynaptic Nerve Terminals

It is not known how the activation of CICR, found in the present study, affects transmitter release from motor nerve terminals during synaptic transmission under the physiological condition. This problem is now under study. Preliminary experiments indicate that the enhancement of end-plate potentials produced by a combination of tetani of different frequencies is blocked by ryanodine (Narita et al., 1998). This is indeed consistent with the previous study that caffeine inhibited the post-tetanic potentiation of evoked release of transmitters, one form of short-term plasticities, at frog motor nerve terminals (Onodera, 1973) and presynaptic terminals in rat hippocampal slices (Lee et al., 1987). The induction of long-term depression in hippocampal neurones was blocked by ryanodine applied externally, but not internally, to postsynaptic neurones (Reyes and Stanton, 1996). Furthermore, Smith and Cunane (1996) recently reported that after the blockade of the fast release of transmitter, ATP, by blocking N-type Ca^{2+} channels with ω-conotoxin GVIA, high frequency stimulation produced ryanodine-sensitive component of transmitter release. Thus, it is likely that CICR plays some roles in the modulation or plasticity of transmitter release. The novel priming and depriming mechanisms of CICR found in frog motor nerve terminals would be more relevant in general for the mechanism of plasticity in central synapses. The priming and depriming of CICR could be one of the mechanisms for conditioning and unconditioning of plasticity. In this context, search for such a mechanism in central synapses may well be necessary.

Another possible role of CICR at the presynaptic terminals would be the activation of oxidative phosphorylation in mitochondria. An electron transfer inhibitor, CN^-, markedly enhanced Ca^{2+}-humps, indicating that mitochondrial Ca^{2+} uptake normally occurs during the tetanus-induced activation of CICR in frog motor nerve terminals. This would imply that the activation of CICR enhances ATP synthesis, since Ca^{2+}-sensitive dehydrogenases play key roles in it (Hansford, 1985; Denton and McCormack, 1990). Furthermore, the oscillations of $[Ca^{2+}]_i$, which were reported to be needed to maintain a high activity of Ca^{2+}-sensitive dehydrogenases (Hajnóczky et al., 1995), were indeed seen occasionally in the present study (data not shown), in the lizard motor nerve terminals (Melamed et al., 1993), and the growth cones of cultured neurones (Gomez et al., 1995; Gu and Spitzer, 1995). Thus, the presynaptic terminals and growth cones, which appear to have high-energy demand, may require CICR to raise mitochondrial Ca^{2+} concentration and its oscillation in addition to impulse-induced Ca^{2+} entry.

This study was supported in part by a Research Project Grant (K. Narita) from Kawasaki Medical School and Grants in Aid for Scientific Research (K. Kuba) from the Japanese Ministry of Education, Science and Culture.

Original version received 15 June 1998 and accepted version received 8 September 1998.

REFERENCES

Baker, A.J., R. Brandes, H.M. Schreur, S.R. Camacho, and M.W. Weiner. 1994. Protein and acidosis alter calcium-binding and fluorescence spectra of the calcium indicator Indo-1. *Biophys. J.* 67: 1646–1654.

Bernardi, P., P. Veronese, and V. Petronilli. 1993. Modulation of the mitochondrial cyclosporin A-sensitive permeability transition pore. *J. Biol. Chem.* 268:1005–1010.

Berridge, M.J. 1993. Inositoltrisphosphate and calcium signalling. *Nature.* 361:315–325.

Bezprozvanny, I., J. Watras, and B.E. Ehrlich. 1991. Bell-shaped calcium response curves of Ins (1,4,5-) P_3- and calcium-gated channels from endoplasmic reticulum of cerebellum. *Nature.* 351: 751–754.

Birks, R., H.E. Huxley, and B. Katz. 1960. The fine structure of the neuromuscular junction of the frog. *J. Physiol. (Camb.).* 150:134–144.

Cseresnyés, Z., A.I. Bustamante, M.G. Klein, and M.F. Schneider. 1997. Release-activated Ca^{2+} transport in neurons of frog sympathetic ganglia. *Neuron.* 19:403–419.

Chiou, C.Y., and M.H. Malagodi. 1975. Studies on the mechanism of action of a new Ca^{2+} antagonist, 8-(*N,N*-diethylamino)octyl 3,4,5-trimethoxybenzoate hydrochloride in smooth and skeletal muscles. *Br. J. Pharmacol.* 53:279–285.

Denton, R.M., and J. McCormack. 1990. Ca^{2+} as a second messenger within mitochondria of the heart and other tissues. *Annu. Rev. Physiol.* 52:451–466.

Duchen, M.R., M. Valdeoolmillos, S.C. O'Neill, and D.A. Eisner. 1990. Effects of metabolic blockade on the regulation of intracellular calcium in dissociated mouse sensory neurones. *J. Physiol. (Camb.).* 424:411–426.

Eckert, R., and D. Tillotson. 1981. Calcium-mediated inactivation of the calcium conductance in caesium-loaded giant neurones of *Aplysia californica*. *J. Physiol. (Camb.).* 314:265–280.

Elmqvist, D., and D.S. Feldman. 1965. Calcium dependence of spontaneous acetylcholine release at mammalian motor nerve terminals. *J. Physiol. (Camb.).* 181:487–497.

Erulkar, S.D., and R. Rahamimoff. 1978. The role of calcium ions in tetanic and post-tetanic increase of miniature end-plate potential frequency. *J. Physiol. (Camb.).* 278:501–511.

Friel, D.D., and R.W. Tsien. 1992. A caffeine- and ryanodine-sensitive Ca^{2+} store in bullfrog sympathetic neurons modulates the effects of Ca^{2+} entry on $[Ca^{2+}]_i$. *J. Physiol. (Camb.).* 450:217–246.

Friel, D.D., and R.W. Tsien. 1994. An FCCP-sensitive Ca^{2+} store in Bullfrog sympathetic neurons and its participation in stimulus-evoked changes in $[Ca^{2+}]_i$. *J. Neurosci.* 14:4007–4024.

Gage, P.W. 1976. Generation of end-plate potentials. *Physiol. Rev.* 56:177–247.

Galli, A., A. Ferroni, L. Bertollini, and M. Mazzanti. 1994. Inactivation of single Ca^{2+} channels in rat sensory neurons by extracellular Ca^{2+}. *J. Physiol. (Camb.).* 477:15–26.

Garaschuk, O., Y. Yaari, and A. Konnerth. 1997. Release and sequestration of calcium by ryanodine sensitive stores in rat hippocampal neurones. *J. Physiol. (Camb.).* 502:13–30.

Gomez, T.M., D.M. Snow, and P.C. Letourneau. 1995. Characterization of spontaneous calcium transients in nerve growth cones and their effect on growth cone migration. *Neuron.* 14:1233–1246.

Grynkiewicz, G., M. Poenie, and R.Y. Tsien. 1985. A new generation of Ca^{2+} indicators with greatly improved fluorescence properties. *J. Biol. Chem.* 260:3440–3450.

Gu, X., and N.C. Spitzer. 1995. Distinct aspects of neuronal differentiation encoded by frequency of spontaneous Ca^{2+} transients. *Nature.* 375:784–787.

Hajnóczky, G., L.D. Robb-Gaspers, M.B. Seitz, and A.P. Thomas. 1995. Decoding of cytosolic calcium oscillations in the mitochondria. *Cell.* 82:415–424.

Hansford, R.G. 1985. Relation between mitochondrial calcium transport and control of energy metabolism. *Rev. Physiol. Biochem. Pharmacol.* 102:1–72.

Heidelberger, R., C. Heinemann, E. Neher, and G. Matthews. 1994. Calcium dependence of the rate of exocytosis in a synaptic terminal. *Nature.* 371:513–515.

Hernández-Cruz, A., A.L. Escobar, and N. Jiménez. 1997. Ca^{2+}-induced Ca^{2+} release phenomena in mammalian sympathetic neurons are critically dependent on the rate of rise of trigger Ca^{2+}. *J. Gen. Physiol.* 109:147–167.

Hua, S.-Y., M. Nohmi, and K. Kuba. 1993. Characteristics of Ca^{2+} release induced by Ca^{2+} influx in cultured bullfrog sympathetic neurones. *J. Physiol. (Camb.).* 464:245–272.

Hunt, J.M., E.M. Silinsky, J.K. Hirsh, D. Ahn, and C. Solsona. 1990. The effects of TMB-8 on acetylcholine release from frog motor nerve: interactions with adenosine. *Eur. J. Pharmacol.* 178:259–266.

Ichas, F., L.S. Jouaville, and J.-P. Mazat. 1997. Mitochondria are excitable organelles capable of generating and conveying electrical and calcium signals. *Cell.* 89:1145–1153.

Katz, B. 1969. The Release of Neural Transmitter Substances. Charles C. Thomas. Springfield, IL.

Katz, B., and R. Miledi. 1968. The role of calcium in neuromuscular facilitation. *J. Physiol. (Camb.).* 195:481–492.

Kijima, H., and S. Kijima. 1982. 'Steady/equilibrium approximation' in relaxation and fluctuation. I. Procedure to simplify first-order reaction. *Biophys. Chem.* 16:181–192.

Konishi, M., A. Olson, S. Hollingworth, and S.M. Baylor. 1988. Myoplasmic binding of fura-2 investigated by steady-state fluorescence and absorbance measurements. *Biophys. J.* 54:1089–1104.

Kuba, K. 1980. Release of calcium ions linked to the activation of potassium conductance in a caffeine-treated sympathetic neurone. *J. Physiol. (Camb.).* 298:251–269.

Kuba, K. 1994. Ca^{2+}-induced Ca^{2+} release in neurones. *Jpn. J. Physiol.* 44:613–650.

Kuba, K., S.-Y. Hua, and T. Hayashi. 1994. A UV laser-scanning confocal microscope for the measurement of intracellular Ca^{2+}. *Cell Calcium.* 16:205–218.

Kuba, K., and S. Nishi. 1976. Rhythmic hyperpolarizations and depolarization of sympathetic ganglion cells induced by caffeine. *J. Neurophysiol.* 39:547–563.

Kuba, K., and S. Takeshita. 1981. Simulation of intracellular Ca^{2+} oscillation in a sympathetic neurone. *J. Theor. Biol.* 93:1009–1031.

Landò, L., and R.S. Zucker. 1994. Ca^{2+} cooperativity in neurosecretion measured using photolabile Ca^{2+} chelators. *J. Neurophysiol.* 72:825–830.

Lee, W.-L., R. Anwyl, and M. Rowan. 1987. Caffeine inhibits post-tetanic potentiation but does not alter long-term potentiation in the rat hippocampal slice. *Brain Res.* 426:250–256.

Llano, I., R. Dipolo, and A. Marty. 1994. Calcium-induced calcium release in cerebellar Purkinje cells. *Neuron.* 12:663–673.

Llinás, R., M. Sugimori, and R.B. Silver. 1992. Microdomains of high calcium concentration at a presynaptic terminal. *Science.* 256:677–679.

Lipscombe, D., D.V. Madison, M. Poenie, H. Reuter, R.W. Tsien, and R.Y. Tsien. 1988. Imaging of cytosolic Ca^{2+} transients arising from Ca^{2+} stores and Ca^{2+} channels in sympathetic neurons. *Neuron.* 1:355–365.

Lockerbie, R.O., and P.R. Gordon-Weeks. 1986. Further characterization of [^{3}H] γ-aminobutyric acid release from isolated neu-

ronal growth cones: role of intracellular Ca^{2+} stores. *Neuroscience.* 17:1257–1266.

Melamed, N., P.J. Helm, and R. Rahamimoff. 1993. Confocal microscopy reveals coordinated calcium fluctuations and oscillations in synaptic boutons. *J. Neurosci.* 13:632–649.

Merritt, J.E., R. Jacob, and T.J. Hallam. 1989. Use of manganese to discriminate between calcium influx and mobilization from internal stores in stimulated human neutrophils. *J. Biol. Chem.* 264: 1522–1527.

Mulkey, R.M., and R.S. Zucker. 1993. Calcium released by photolysis of DM-nitrophen triggers transmitter release at the crayfish neuromuscular junction. *J. Physiol. (Camb.).* 462:243–260.

Narita, K., K. Ochi, T. Akita, and K. Kuba. 1998. Short term plasticity caused by Ca^{2+} induced Ca^{2+} release in frog motor nerve terminals. *Neurosci. Res. Suppl.* 22:S97.

Neher, E., and A.G. Augustine. 1992. Calcium gradients and buffers in bovine chromaffin cells. *J. Physiol. (Camb.).* 450:273–301.

Nohmi, M., C. Liu, and K. Kuba. 1994. Mitochondrial Ca^{2+}-induced Ca^{2+} release in response to cell membrane depolarization in rabbit autonomic neurones. *Neurosci. Res. Suppl.* 19:S27.

Ohta, Y., and K. Kuba. 1980. Inhibitory action of Ca^{2+} on spontaneous acetylcholine release at motor nerve terminals in a high K^+ solution. *Pflügers Arch.* 386:29–34.

Onodera, K. 1973. Effect of caffeine on the neuromuscular junction of the frog, and its relation to external calcium concentration. *Jpn. J. Physiol.* 23:587–597.

Osanai, M., S. Suzuki, N. Suzuki, K. Kuba, and H. Kijima. 1996. Presynaptic Ca^{2+}-imaging at the frog neuromuscular junction. *Neurosci. Res.* 20:S36.

Peng, Y.-Y. 1996. Ryanodine-sensitive component of calcium transients evoked by nerve firing at presynaptic nerve terminals. *J. Neurosci.* 16:6703–6712.

Peng, Y.-Y., and R.S. Zucker. 1993. Release of LHRH is linearly related to the time integral of presynaptic Ca^{2+} elevation above a threshold level in bullfrog sympathetic ganglia. *Neuron.* 10:465–473.

Peper, K., F. Dreyer, C. Sandri, K. Akert, and H. Moor. 1974. Structure and ultrastructure of the frog motor end-plate. A freeze-etching study. *Cell Tissue Res.* 149:437–455.

Ravin, R., M.E. Spira, H. Parnas, and I. Parnas. 1997. Simultaneous measurement of intracellular Ca^{2+} and asynchronous transmitter release from the same crayfish bouton. *J. Physiol. (Camb.).* 501: 252–262.

Reyes, M., and P.K. Stanton. 1996. Induction of hippocampal long-term depression requires release of Ca^{2+} from separate presynaptic and postsynaptic intracellular stores. *J. Neurosci.* 16:5951–5960.

Szabó, I., and M. Zoratti. 1993. The mitochondrial permeability transition pore may comprise VDAC molecules. *FEBS Lett.* 330: 201–205.

Schweizer, F.E., H. Betz, and A.G. Augustine. 1995. From vesicle docking to endocytosis: intermediate reactions of exocytosis. *Neuron.* 14:689–696.

Südhof, T.C. 1995. The synaptic vesicle cycle: a cascade of protein–protein interactions. *Nature.* 375:645–653.

Smith, A.B., and T.C. Cunnane. 1996. Ryanodine-sensitive calcium stores involved in neurotransmitter release from sympathetic nerve terminals of the guinea-pig. *J. Physiol. (Camb.).* 497:657–664.

Sutko, J.L., J.T. Willerton, G.H. Templeton, L.R. Jones, and H.R. Besch. 1979. Ryanodine: its alteration of cat papillary muscle contractile state and responsiveness to inotropic interventions and a suggested mechanism of action. *J. Pharmacol. Exp. Ther.* 209:961–964.

Tanabe, N., and H. Kijima. 1992. Ca^{2+}-dependent and -independent components of transmitter release at the frog neuromuscular junction. *J. Physiol. (Camb.).* 455:271–289.

Thayer, S.A., L.D. Hirning, and R.J. Miller. 1988. The role of caffeine-sensitive calcium stores in the regulation of the intracellular free calcium concentration in rat sympathetic neurons *in vitro. Mol. Pharmacol.* 34:664–673.

Thayer, S.A., and R.J. Miller. 1990. Regulation of the intracellular free calcium concentration in single rat dorsal root ganglion neurones *in vitro. J. Physiol. (Camb.).* 425:85–115.

Tóth, P.Y., T.L. Török, and K. Magyar. 1990. Depolarization promotes caffeine induced [^{3}H]-noradrenaline release in calcium-free solution from peripheral sympathetic nerves. *Cell Calcium.* 11:557–563.

Usachev, Y., A. Shmigol, N. Pronchuk, P. Kostyuk, and A. Verkhratsky. 1993. Caffeine-induced calcium release from internal stores in cultured rat sensory neurons. *Neuroscience.* 57:845–859.

Yoshizaki, K., T. Hoshino, M. Sato, H. Koyano, M. Nohmi, S.-Y. Hua, and K. Kuba. 1995. Ca^{2+}-induced Ca^{2+} release and its activation in response to a single action potential in rabbit otic ganglion cells. *J. Physiol. (Camb.).* 486:177–187.

Zucker, R.S. 1996. Exocytosis: a molecular and physiological perspective. *Neuron.* 17:1049–1055.